Am J Cancer Res 2020;10(10):3382-3394
www.ajcr.us /ISSN:2156-6976/ajcr0118182

Original Article

Novel genetic variants of *PIP5K1C* and *MVB12B* of the endosome-related pathway predict cutaneous melanoma-specific survival

Guiqing Lu[1,2,3*], Bingrong Zhou[2,3*], Yuanmin He[2,3], Hongliang Liu[2,3], Sheng Luo[4], Christopher I Amos[5], Jeffrey E Lee[6], Keming Yang[7], Abrar Qureshi[8], Jiali Han[9,10], Qingyi Wei[2,3,11]

[1]Department of Dermatology, BenQ Medical Center, The Affiliated BenQ Hospital of Nanjing Medical University, Nanjing 210019, Jiangsu, China; [2]Duke Cancer Institute, Duke University Medical Center, Durham, NC 27710, USA; [3]Department of Population Health Sciences, Duke University School of Medicine, Durham, NC 27710, USA; [4]Department of Biostatistics and Bioinformatics, Duke University School of Medicine, Durham, NC 27710, USA; [5]Institute for Clinical and Translational Research, Baylor College of Medicine, Houston, TX 77030, USA; [6]Department of Surgical Oncology, The University of Texas M.D. Anderson Cancer Center, Houston, TX 77030, USA; [7]Department of Nutrition, Harvard T.H. Chan School of Public Health, Boston, MA, USA; [8]Department of Dermatology, Warren Alpert Medical School, Brown University, Providence, RI 02903, USA; [9]Channing Division of Network Medicine, Department of Medicine, Brigham and Women's Hospital, Boston, MA 02115, USA; [10]Department of Epidemiology, Fairbanks School of Public Health, Indiana University, Indianapolis, IN 46202, USA; [11]Department of Medicine, Duke University School of Medicine, Durham, NC 27710, USA. [*]Equal contributors.

Received July 14, 2020; Accepted July 22, 2020; Epub October 1, 2020; Published October 15, 2020

Abstract: Endosomes regulate cell polarity, adhesion, signaling, immunity, and tumor progression, which may influence cancer outcomes. Here we evaluated associations between 36,068 genetic variants of 228 endosome-related pathway genes and cutaneous melanoma disease-specific survival (CMSS) using genotyping data from two previously published genome-wide association studies. The discovery dataset included 858 CM patients with 95 deaths from The University of Texas MD Anderson Cancer Center, and the replication dataset included 409 CM patients with 48 deaths from the Nurses' Health Study (NHS) and the Health Professionals Follow-up Study (HPFS). In multivariate Cox proportional hazards regression analysis, we found that two novel SNPs (*PIP5K1C* rs11666894 A>C and *MVB12B* rs12376285 C>T) predicted CMSS, with adjusted hazards ratios of 1.47 (95% confidence interval = 1.15-1.89 and P = 0.002) and 1.73 (1.30-2.31 and 0.0002), respectively. Combined analysis of risk genotypes of these two SNPs revealed a dose-dependent decrease in CMSS associated with an increased number of risk genotypes (P_{trend} = 0.0002). Subsequent expression quantitative trait loci (eQTL) analysis revealed that *PIP5K1C* rs11666894 was associated with mRNA expression levels in lymphoblastoid cell lines from 373 European descendants (P<0.0001) and that *MVB12B* rs12376285 was associated with mRNA expression levels in cultured fibroblasts from 605 European-Americans (P<0.0001). Our findings suggest that novel genetic variants of *PIP5K1C* and *MVB12B* in the endosome-related pathway genes may be promising prognostic biomarkers for CMSS, but these results need to be validated in future larger studies.

Keywords: Genome-wide association study, cutaneous melanoma-specific survival, endosome pathway, single-nucleotide polymorphism, immunity

Introduction

Cutaneous melanoma (CM) is the most aggressive skin cancer, ranking the fifth most common fatal malignancy among males and the sixth among females in the United States [1]. In 2019, an estimated 96,480 new CM cases were diagnosed in the United States, accounting for about 5.5% of all new cancer cases, of whom 7,230 patients died of the disease [2]. Although targeted therapy and immunotherapy have remarkably improved outcomes in patients with CM over the past decade, prognosis for patients with advanced or metastatic CM is still very poor, with five-year overall survival (OS) of 30% to 40% [3, 4]. Several clinical character-

istics have been reported to affect the prognosis of CM patients, such as tumor stage, Breslow thickness, and ulceration [5], but the prognosis based on these variables still has limited accuracy. Recently, genetic factors such as single nucleotide polymorphisms (SNPs) have been shown to affect CM disease-specific survival (CMSS) [6]. Therefore, identifying the roles of these genetic factors in CM survival may improve personalized management and treatment of CM patients.

Studies have suggested that some SNPs affect protein functions by various mechanisms, including gene expression regulation, and play an important role in molecular pathogenesis [7]. Genome-wide association studies (GWASs) have advanced the investigation of complex disease genetics and identified thousands of disease-associated SNPs [8]. However, associations detected by GWASs do not yield specific gene targets or provide biological mechanisms, because the SNPs identified and reported are often located in intragenic regions. However, there is a growing realization that the majority of phenotypic variation remains unaccounted for, and much of the heritability remains unexplained [9]. From identification of an association to a functional discovery, incorporating biological insights via explicit modeling of underlying biological pathways is essential and has become the focus of recent research [10]. To date, few novel and functional SNPs have been identified to be associated with CM prognosis in the reported GWASs. In addition, most of the identified SNPs failed to reach the rigorous genome-wide significance level, and >90% of disease-associated SNPs are located in non-protein-coding regions of the genome, of which many are far away from the nearest known gene [11]. However, in the post-GWAS era, one can use a hypothesis-driven strategy to identify functional genetic variants in targeted biological pathway genes through their associations with CMSS at a pathway level, and this can be achieved with publicly available genotyping data from multiple previously-published GWAS datasets [10].

The endosomal system is a complex network of membrane-bound compartments, which regulates cell polarity, adhesion, signaling, immunity, and tumor progression, and may influence tumor progression and prognosis of cancer patients. Studies have suggested that cancer development and tumor progression involve endosomal upregulation of oncogenic signalling, likely through defective trafficking of growth factor receptors, increased recycling, or decreased degradation [12, 13]. For example, the endosome plays an important role in carcinogenesis of melanocytes through the interaction between melanoma oncogene *MITF* and macrophage [14]. A multiepitope tissue analysis revealed that endosomal translocation and hence metalloproteinase ADAM10 activation were key steps in the transformation of melanocytes and melanoma development [15]. On the other hand, some animal studies have indicated that Rab7 GTPase, a late endosome/lysosome-associated small GTPase, regulates tumorigenesis and mediates growth and metastasis of melanoma under the control of the endosomal/lysosomal system in lysosomal acid lipase-deficient mice [16]. Furthermore, the endosome participates in hypoxia-induced melanoma metastasis through the upregulated expression of Rab5 in another mouse model [17].

In humans, the endosomal system as the pathogen entry-point is equipped to process and display the foreign fragments to elicit an effective immune response [18]. In counteracting with deleterious effects of tumor agents, antigen-presenting cells (APCs) rewire their endosomal pathway to optimize the presentation of antigens to the immune system, while canonical presentation of exogenous antigens by major histocompatibility complex (MHC) class II (residing in the late endosomal compartment termed the MIIC) to CD4+ T cells is transiently supplemented by cross-presentation on MHC class I to CD8+ T cells [19, 20]. These indicate that the endosomes are involved in CM carcinogenesis, metastasis, and immune response. Therefore, we hypothesize that genetic variants of endosome-related pathway genes are associated with CM survival. We tested this hypothesis using genotyping data from publicly available melanoma GWAS datasets.

Materials and methods

Study populations

The discovery dataset included genotyping and survival data on 858 non-Hispanic white patients with CM recruited at The University of Texas MD Anderson Cancer Center (MDACC)

GWAS study derived from a hospital-based case-control study. The available demongraphic and clinical information included age, sex, Breslow thickness, metastasis, ulceration of tumor, mitotic rate, and survival outcome. The replication dataset comprised genotyping and survival data on an additional 409 participants with invasive CM from two cohort studies: the Nurses' Health Study (NHS) and the Health Professionals Follow-up Study (HPFS). There were some differences in age and sex distributions between the two datasets, e.g., the proportion of young patients (≤50 years) was 43.24% in the MDACC dataset and 17.60% in the Harvard dataset. Also, the percentage of female participants was 42.19% and 66.26% in the MDACC and Harvard datasets, respectively. Subject selection and data collection for both discovery and replication datasets have been published in detail elsewhere [21, 22]. All patients in both studies provided written informed consent under a research protocol approved by the Institutional Review Boards of the MDACC, Brigham and Women's Hospital, and the Harvard T.H. Chan School of Public Health, and those of participating registries as required.

Gene selection and SNP genotyping

The genes involved in the endosome-related pathway were selected from the Molecular Signatures Database of Gene Set Enrichment Analysis (GSEA) website (http://software.broadinstitute.org/gsea/msigdb/search.jsp), using the keyword "endosome". After the removal of 62 duplicated genes, six genes in the X chromosome and one pseudogene, we used the 228 endosome-related pathway genes located on the autosomes as candidate genes for further analysis (Table S1). In the MDACC GWAS dataset, genomic DNA was extracted from whole blood cells and used for genotyping in the Illumina HumanOmni-Quad_v1_0_B array. The genotyping data are available at the National Center for Biotechnology Information Database of Genotypes and Phenotypes (dbGaP Study Accession: phs000187.v1.p1). Genome-wide imputation was performed based on the CEU data from 1000 Genomes Project (phase I v2), utilizing the MACH software (March 2010 release). We used both typed (with a genotyping success rate of 95% and a Hardy-Weinberg equilibrium P value of 10^{-5}) and imputed (r^2>0.8) common SNPs (with a minor allele frequency of 0.05) within ± 2 kilobase flanking regions of these endosome-related pathway genes. In the validation GWAS dataset, whole blood DNA samples were used for genotyping with the HumanHap610, Affymetrix 6.0, and Illumina HumanHap550 arrays, and imputation was based on haplotype information from 1000 Genomes project CEU data (2012 release), by applying MACH with quality control similar to that used for the MDACC GWAS dataset.

Statistical methods

We first assessed associations between all available SNPs in endosome-related pathway genes and CMSS in a single-locus Cox proportional hazards regression analysis. Then we performed multivariate Cox proportional hazards regression analyses with adjustment for available covariates. We used the less stringent Bayesian false-discovery probability (BFDP) for multiple testing correction, because the vast majority of the SNPs under investigation are in high linkage disequilibrium (LD), and we intended to identify all possible functional SNPs with a relaxed correction method. We subsequently evaluated cumulative effects of identified SNPs and also showed the associations between CM survival probability and combined risk genotypes via Kaplan-Meier (KM) survival curves. The receiver operating characteristic (ROC) curve and time-dependent area under the curve (AUC) were used to compare the prediction accuracy of models including both clinical and genetic variables on CMSS. To evaluate the correlation between the identified SNPs and mRNA expression levels of their genes, we performed expression quantitative trait loci (eQTL) analyses using the mRNA expression data of lymphoblastoid cell-lines derived from the 373 European-descendants in the 1,000 Genomes Project, and 483 cultured fibroblasts obtained from the genotype-tissue expression (GTEx) project database. Other details are presented in Supplementary Methods.

Results

Patient features

Baseline characteristics of CM patients from both GWAS datasets have been described else-

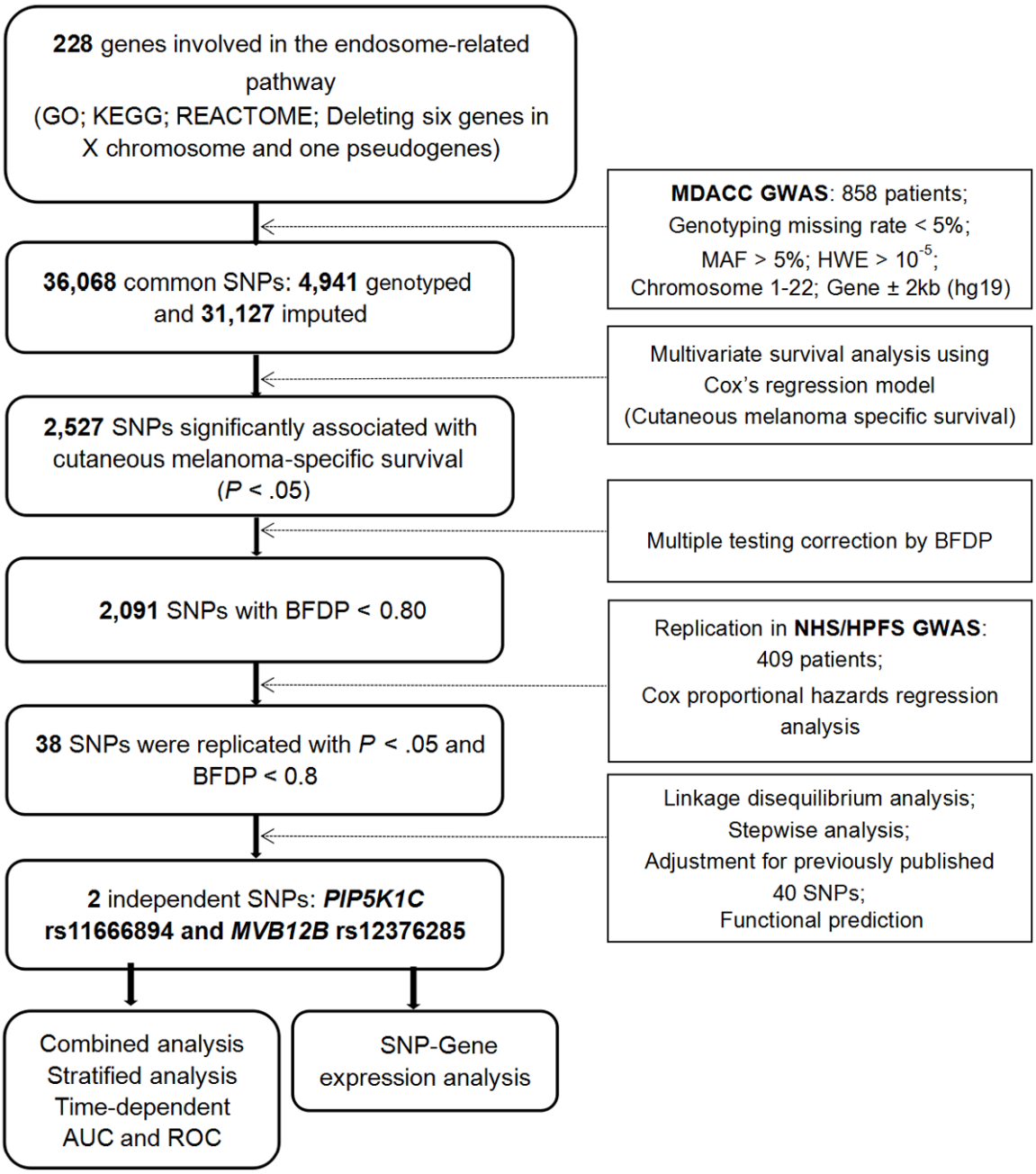

Figure 1. The flowchart of the study. Abbreviations: SNP, single-nucleotide polymorphism; MDACC, The University of Texas MD Anderson Cancer Center; GWAS, genome-wide association study; MAF, minor allele frequency; HWE, Hardy Weinberg equilibrium; BFDP, Bayesian false-discovery probability; NHS/HPFS, the Nurses' Health Study/Health Professionals Follow-up Study; AUC, area under curve; ROC, receiver operating characteristic.

where [21, 22]. The MDACC dataset had demographic and clinical information about age, sex, tumor stage, Breslow thickness, ulceration and mitotic rate, while the NHS/HPFS dataset had only age, sex, and survival outcome. Compared with the NHS/HPFS dataset, patients diagnosed in the MDACC dataset were younger (82.4% vs. 56.8% for >50 years) and more likely to be male (33.8 vs. 57.8%). The MDACC dataset included CM cases of different stages diagnosed at an outpatient clinic, while the NHS/HPFS dataset included CM cases likely at an earlier stage I/II from the active follow-up of healthy populations. For these reasons, the median follow-up was shorter among MDACC patients, compared with NHS/HPFS patients

Table 1. Two independent SNPs identified by multivariate Cox proportional hazards regression analysis in the MDACC melanoma GWAS dataset

Parameter	Category[1]	Frequency	HR (95% CI)[2]	*P*[2]	HR (95% CI)[3]	*P*[3]
Age	≤50/>50	371/487	1.40 (0.89-2.20)	0.145	2.36 (1.35-4.13)	0.003
Sex	Female/Male	362/496	1.62 (1.01-2.60)	0.045	1.35 (0.80-2.28)	0.263
Regional/distantmetastasis	No/Yes	709/149	3.86 (2.51-5.92)	<0.0001	12.41 (6.77-22.76)	<0.0001
Breslow thickness (mm)	≤1/>1	347/511	1.19 (1.12-1.25)	<0.0001	1.26 (1.17-1.36)	<0.0001
Ulceration	No/Yes	681/155	2.40 (1.56-3.71)	<0.0001	3.40 (2.00-5.78)	<0.0001
Mitotic rate (/mm^2)	≤1/>1	275/583	2.53 (1.24-5.15)	0.011	2.68 (1.19-6.03)	0.017
PIP5K1C rs11666894 A>C	AA/AC/CC	240/447/171	1.50 (1.09-2.06)	0.013	1.76 (1.21-2.56)	0.003
MVB12B rs12376285 C>T	CC/CT/TT	597/237/24	1.67 (1.13-2.46)	0.010	1.78 (1.13-2.81)	0.013

Abbreviations: SNP, single-nucleotide polymorphism; MDACC, The University of Texas MD Anderson Cancer Center; HR, hazards ratio; CI, confidence interval. [1]The "category" was used as the reference; [2]Stepwise analysis included age, sex, regional/distant metastasis, Breslow thickness, ulceration, mitotic rate and SNPs; [3]Forty published SNPs were used for post-stepwise adjustment. Four SNPs were reported in previous publication (PMID: 25953768); Three SNPs was reported in the previous publication (PMID: 25628125); Four SNPs were reported in the previous publication (PMID: 25243787); Two SNPs were reported in the previous publication (PMID: 26575331); Two SNPs were reported in the previous publication (PMID: 30734280); Three SNPs were reported in the previous publication (PMID: 30596980); Three SNPs were reported in the previous publication (PMID: 29313974); Two SNPs were reported in the previous publication (PMID: 29088810); Four SNPs were reported in the previous publication (PMID: 28796414); One SNPs were reported in the previous publication (PMID: 28542949); Two SNPs were reported in the previous publication (PMID: 28499756); Three SNPs were reported in the previous publication (PMID: 27914105); Three SNPs were reported in the previous publication (PMID: 27578485).

(81.1 months vs. 179.0 months); however, death rates during follow-up were similar: (95/858 or 11.1% and 48/409 or 11.7%), respectively (Table S2). Because none of the principal components based on the GWAS genotyping data was significantly associated with CM survival, suggesting no significant population stratification in either the MDACC or NHS/HPFS datasets, we did not adjust for the principal components in either the discovery or replication analyses.

Associations between SNPs in the endosome-related pathway genes and CMSS

After removal of 62 duplicated genes, one pseudogene (*AC034102.1*), and six genes on the X chromosome (i.e., *MSN*, *SNX12*, *IL2RG*, *IQSEC2*, *SH3KBP1*, *MTM1* because no standard statistics have been established for sex-specific analysis), 228 endosome-related genes remained for further analysis. As shown in **Figure 1**, a total of 4,941 genotyped and 31,127 imputed SNPs were extracted for 228 endosome-related pathway genes from the MDACC discovery dataset. The associations between these SNPs and CMSS were assessed in a single-locus analysis using Cox regression; 2,527 SNPs were found to be associated with CMSS (P<0.05) in an additive genetic model; and 2,091 SNPs remained noteworthy after multiple testing correction by BFDP <0.8. With subsequent replication in the NHS/HPFS dataset, only 38 SNPs remained significantly associated with CMSS, which are located in five genes (33 SNPs in *MVB12B*, two in *PIP5K1C*, and one each in *AGAP1*, *IQSEC3*, and *IQSEC1*) (Table S3) and remained significant in the meta-analysis of the two datasets without obvious heterogeneity (Table S4). In the LD analysis of these 38 significant SNPs, we found two SNPs in *PIP5K1C* and 33 SNPs in *MVB12B* to be in high LD (Figure S1). The remaining SNPs were further tested for their independence in predicting CMSS.

Two independent SNPs predict CMSS

To identify SNPs with independent effects, we conducted stepwise multivariate Cox regression analyses to assess the effects of 38 validated SNPs on CMSS in the MDACC dataset, but not in the NHS/HPFS dataset that did not contain the same clinical covariates as the MDACC dataset did. Three SNPs (rs11666894, rs12376285, and rs77278014) in three genes (*PIP5K1C*, *FAM125B,* and *IQSEC1*, respectively) remained significantly associated with CMSS (P<0.05) in the presence of clinical covariates. After we expanded this prediction model with adjustment for an additional 40 previously reported survival-associated SNPs in the same MDACC GWAS dataset, we found that two SNPs (*PIP5K1C* rs11666894 A>C and *MVB-12B* rs12376285 C>T) remained significantly associated with CMSS (P = 0.003 and 0.013,

Table 2. Meta-analysis of the two independent SNPs in endosome-related pathway genes identified from two previously published melanoma GWAS datasets

SNP	Allele[1]	Gene	Discovery-MDACC (n = 858)				Validation-NHS/HPFS (n = 409)				Combined-analysis (n = 1267)			
			EAF	HR (95% CI)	*P*[2]	BFDP	EAF	HR (95% CI)	*P*[3]	BFDP	P_{het}	I^2	HR (95% CI)	*P*[4]
rs12376285[$]	C>T	*MVM12B*	0.17	1.75 (1.19-2.56)	0.004	0.434	0.19	1.71 (1.10-2.66)	0.017	0.691	0.938	0	1.73 (1.30-2.31)	1.87×10^{4}
rs11666894[$]	A>C	*PIP5K1C*	*0.46*	1.40(1.03-1.91)	0.033	0.771	0.49	1.61(1.08-2.44)	0.022	0.709	0.593	0	1.47 (1.15-1.89)	0.002

[1]Reference allele>effect allele; [2]Adjusted for age, sex, Breslow thickness, distant/regional metastasis, ulceration and mitotic rate in the additive model; [3]Adjusted for age and sex in the additive model; [4]Meta-analysis in the fix-effect model; [$]Imputed SNP; Abbreviations: SNP, single-nucleotide polymorphism; GWAS, genome-wide association study; MDACC, MD Anderson Cancer Center; EAF, effect allele frequency; HR, hazards ratio; CI, confidence interval; BFDP, Bayesian false-discovery probability; P_{het}, *P* value for heterogeneity by Cochrane's Q test; MVB12B, multivesicular body subunit 12B; PIP5K1C, phosphatidylinositol-4-phosphate 5-kinase type 1 gamma.

Table 3. Joint-analysis of the two identified independent SNPs in endosome-related pathway genes and CMSS of patients in the MDACC dataset, the NHS/HPFS dataset, and the MDACC and NHS/HPFS pooled dataset

Genotype	MDACC (n = 858)				NHS/HPFS (n = 409)				MDACC+NHS/HPFS (n = 1267)			
	Frequency		Multivariate analysis[1]		Frequency		Multivariate analysis[2]		Frequency		Multivariate analysis[3]	
	All	Death (%)	HR (95% CI)	*P*	All	Death (%)	HR (95% CI)	*P*	All	Death (%)	HR (95% CI)	*P*
PIP5K1C rs11666894 A>C												
AA	240	17 (7.08)	1.00		98	8 (8.16)	1.00		338	25 (7.40)	1.00	
AC	447	54 (12.08)	1.70 (0.96-2.99)	0.068	208	21 (10.10)	1.28 (0.56-2.90)	0.556	655	75 (11.45)	1.59 (1.01-2.51)	0.044
CC	171	24 (14.04)	2.03 (1.05-3.90)	0.035	103	19 (18.45)	2.42 (1.06-5.54)	0.037	274	43 (15.69)	2.18 (1.33-3.57)	0.002
Trend test				0.033				0.022				0.002
AC+CC	618	78 (12.62)	1.79 (1.03-3.08)	0.040	311	40 (12.86)	1.65 (0.77-3.54)	0.197	929	118 (12.70)	1.77 (1.15-2.72)	0.010
MVB12B rs12376285 C>T												
CC	597	61 (10.22)	1.00		265	21 (7.92)	1.00		862	82 (9.51)	1.00	
CT	237	29 (12.24)	1.48 (0.94-2.32)	0.093	129	26 (20.16)	2.60 (1.46-4.63)	0.001	366	55 (15.03)	1.55 (1.10-2.18)	0.012
TT	24	5 (20.83)	5.28 (2.00-13.95)	0.001	15	1 (6.67)	0.81 (0.11-6.00)	0.833	39	6 (15.38)	1.55 (0.67-3.56)	0.302
Trend test				0.004				0.017				0.014
CT+TT	261	34 (13.03)	1.63 (1.06-2.51)	0.027	144	27 (18.75)	2.41 (1.36-4.26)	0.003	405	61 (15.06)	1.55 (1.11-2.16)	0.010
Number of risk genotypes[4]												
0	165	8 (4.85)	1.00		60	4 (6.67)	1.00		225	12 (5.33)	1.00	
1	507	62 (12.23)	2.58 (1.16-5.72)	0.020	243	21 (8.64)	1.31 (0.45-3.84)	0.618	750	83 (11.07)	2.04 (1.11-3.74)	0.021
2	186	25 (13.44)	3.77 (1.61-8.87)	0.002	106	23 (21.70)	3.45 (1.19-10.03)	0.023	292	48 (16.44)	3.09 (1.64-5.82)	5E-04
Trend test				0.002				0.001				2E-04
0-1	672	70 (10.42)	1.00		303	25 (8.25)	1.00		975	95 (9.74)	1.00	
2	186	25 (13.44)	1.69 (1.06-2.70)	0.027	106	23 (21.70)	2.76 (1.56-4.88)	0.001	292	48 (16.44)	1.71 (1.21-2.43)	0.002

[1]Adjusted for age, sex, Breslow thickness, distant/regional metastasis, ulceration and mitotic rate in the MDACC dataset; [2]Adjusted for age and sex in the NHS/HPFS dataset; [3]Adjusted for age and sex in the combined MDACC and NHS/HPFS dataset; [4]Risk genotypes include *PIP5K1C* rs11666894 AC+CC and *MVB12B* rs12376285 CT+TT.

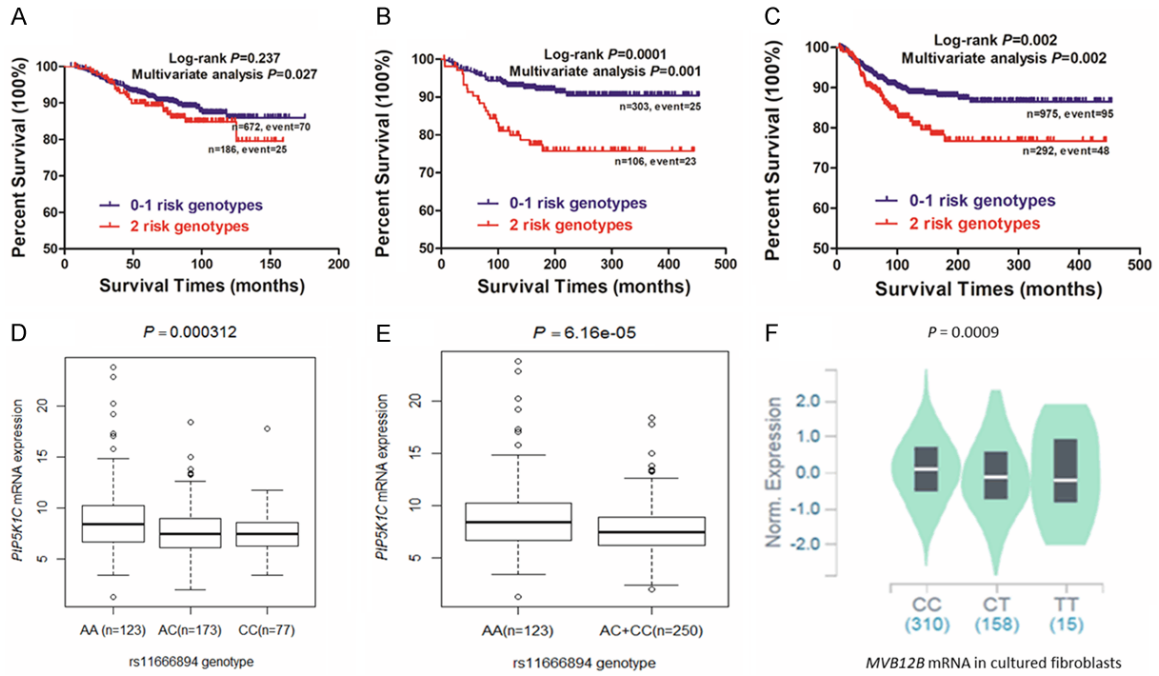

Figure 2. Two independent SNPs in endosome-related pathway genes predict cutaneous melanoma survival and eQTL analysis for them. Kaplan-Meier survival curves of CM patients by the combined risk genotypes of *PIP5K1C rs11666894* and *MVB12B rs12376285*: dichotomized 0-1 risk genotype group and 2 risk genotypes group in the MDACC dataset (A), the NHS/HPFS dataset (B) and combined MDACC and NHS/HPFS dataset (C). The correlation of *rs11666894* and *PIP5K1C* mRNA expression from the 1000 Genomes Project in an additive model (D) and an dominant model (E). The correlation of *rs12376285* and *MVB12B* mRNA expression in cultured fibroblasts from the GTEx (F). Abbreviations: SNP, single-nucleotide polymorphism; eQTL, expression quantitative trait loci; CMSS, cutaneous melanoma-specific survival; MDACC, The University of Texas MD Anderson Cancer Center; NHS, the Nurses' Health Study; HPFS, the Health Professionals Follow-up Study; GTEx, Genotype-Tissue Expression project.

respectively) (**Table 1**). The results of meta-analysis of these two independent SNPs in each dataset are shown in **Table 2** without heterogeneity across datasets. Specifically, as shown in **Table 3**, we found that *PIP5K1C* rs11666894 C and *MVB12B* rs12376285 T alleles were both associated with a poor CMSS in the MDACC dataset (P_{trend} = 0.033 and 0.004, respectively), with similar results in the NHS/HPFS dataset (P_{trend} = 0.022 and 0.017, respectively) and in the combined MDACC and NHS/HPFS dataset (P_{trend} = 0.002 and 0.014, respectively) (**Table 3**). For visual presentation, all of the identified SNPs in the present study (including the two independent SNPs) are depicted in a Manhattan plot (Figure S2), and additional regional association plots for these two SNPs are displayed in Figure S3.

Survival of CM patients with combined risk genotypes

To investigate the joint effect of the two independent SNPs on CMSS, we combined the risk genotypes of *PIP5K1C* rs11666894 AC+CC and *MVB12B* rs12376285 CT+TT. We divided the patients into three groups according to their number of risk genotypes (NRG), and the trend test in each dataset revealed a statistically significant dose-response effect of NRG on survival. That is, the higher NRG, the worse survival in the MDACC dataset (P_{trend} = 0.002), the NHS/HPFS dataset (P_{trend} = 0.001), and the MDACC and NHS/HPFS combined dataset (P_{trend} = 0.0002) after adjustment for covariates, wherever appropriate (**Table 3**).

We also dichotomized the patients into 0-1 and 2 NRG groups. As illustrated in **Table 3**, compared with the 0-1 NRG group, the 2-NRG group had a significantly worse CMSS in all datasets: for MDACC (HR = 1.69; 95% CI = 1.06-2.70, *P* = 0.027), NHS/HPFS (HR = 2.76; 95% CI = 1.56-4.88, *P* = 0.001) and the combined MDACC and NHS/HPFS dataset (HR = 1.71; 95% CI = 1.21-2.43, *P* = 0.002). We used Kaplan-Meier survival curves to illustrate the

association between NRG and CMSS (**Figure 2A-C**).

Stratified analyses for the effect of combined risk genotypes on CMSS

Next we performed a stratification analysis to evaluate whether the combined effect of risk genotypes on CMSS was modified by other covariables, including age, sex, tumor stage, Breslow thickness, ulceration, and mitotic rate in the MDACC dataset, but only age and sex in the NHS/HPFS dataset. Compared with those with 0-1 risk genotypes, patients with 2 risk genotypes had a significantly worse survival, particularly evident in the subgroups of those aged >60 years, males, no regional/distant metastasis, Breslow thickness >1 mm, no ulceration, and mitotic rate >1 in the MDACC dataset, and the subgroup aged >60 and female in the NHS/HPFS dataset. Furthermore, there was a significant interaction between risk genotypes and regional/distant metastasis (P = 0.010), but not among the other subgroups (Table S5).

ROC curves and time-dependent AUC for CMSS prediction

To further evaluate the predictive value of the two independent SNPs, we used time-dependent AUC of the ROC curves for CM patients in the presence of available covariates (i.e., age, sex, tumor stage, Breslow thickness, ulceration, and mitotic rate). As shown in Figure S4A-F for the ROC curves, compared with clinical pathologic variables alone, we found that the combination of clinical pathologic variables and risk genotypes improved prediction performance of the five-year CMSS by 1.40% (AUC = 63.60% to 65.00%, P = 0.500) in the combined MDACC and NHS/HPFS dataset, without reaching statistical significance.

In silico functional validation of the two independent SNPs

To further explore the molecular mechanisms underlying the associations between the two independent SNPs and CMSS, we performed additional eQTL analysis for correlations between risk genotypes of the two independent SNPs and their corresponding mRNA expression levels in 373 normal lymphoblastoid cell lines from the 1000 Genomes Project database. We found that the rs11666894 C allele showed a significant correlation with decreased mRNA expression levels of *PIP5K1C* in both additive and dominant models ($P = 3.12\times10^{-4}$ and $P = 6.16\times10^{-5}$, respectively) (**Figure 2D-E**) but not in a recessive model (P = 0.076) (Figure S5D). Meanwhile, we found no evidence of a correlation between *MVB12B* mRNA expression levels and rs12376285 genotypes from the 1000 Genomes Project (Figure S5A-C). Additionally, we performed eQTL analysis by extracting data from the GTEx Project, which has data on both genotypes and mRNA expression for *PIP5K1C* rs11666894 and *MVB12B* rs12376285 obtained from cultured donor fibroblasts. The results showed that the rs12376285 T allele was significantly correlated with lower mRNA expression levels of *MVB12B* ($P = 9.100\times10^{-4}$) (**Figure 2F**) but not the *PIP5K1C* rs11666894 allele (P = 0.880) (Figure S5E).

Finally, we evaluated the associations of mRNA expression levels of *PIP5K1C* and *MVB12B* in different cancers with survival, based on The Human Protein Atlas database (www.proteinatlas.org). As shown in KM survival curves (Figure S6A-E), higher expression levels of *PIP5K1C* mRNA were significantly associated with longer survival in patients with cancers of endometrium, cervix, pancreas, or kidney, indicating that *PIP5K1C* expression is a prognostic marker for survival in other cancer patients as well. Similarly, a higher expression level of *MVB12B* mRNA was significantly associated with a longer survival of patients with pancreatic cancer.

Discussion

To date, a limited number of susceptibility loci in a few pathways have been identified for predicting CM survival. To our knowledge, the present study is the first post GWAS-based pathway analysis to evaluate the associations between genetic variants in the endosome-related pathway genes and CM survival. We found that two novel independent SNPs, *PIP5K1C* rs11666894 A>C and *MVB12B* rs12376285 C>T, independently or jointly modulated survival of Caucasian CM patients. Specifically, *PIP5K1C* rs11666894 C and *MVB12B* rs12376285 T alleles were both identified as prognostic risk alleles for CMSS, and their combined NRG was significantly associated with worse CMSS. Furthermore, the prognostic risk alleles were significantly associated with decreased mRNA expression in lymphoblastoid cell lines or cul-

tured fibroblasts. These results suggest potential biological roles of endosome-related pathway genes in CM survival.

PIP5K1C, located on chromosome 19p13.3, encodes phosphatidylinositol-4-phosphate 5-kinase type-1 gamma; this kinase has been reported in the formation of membrane contact sites among various organelles, including the plasma membrane, endoplasmic reticulum, and endolysosomal system. This kinase also performs spatial and temporal control of phosphatidylinositol (4,5)-bisphosphate (PIP2) synthesis as well as regulates E-cadherin cell-cell contacts and growth factor-stimulated dendritic cell (DC) migration; these findings suggest that *PIP5K1C* regulates key steps in metastasis [23-25]. PIP5K1C has been known to have immune-regulatory effects via the modulation of neutrophil polarization and infiltration [26]. PIP5K1C may also be a critical regulator of T-cell activation through PIP2, which in turn regulates T-cell receptor (TCR) signaling [27, 28], and E-cadherin, which plays a critical role in the action of cytotoxic T lymphocytes (CTLs) in TCR-mediated killing by interacting with and directing exocytosis of lytic granules to the cancer cell surface at the immunological synapse [29, 30].

To date, no studies on associations of *PIP5K1C* variants with cancer risk have been reported. However, a case-control association study showed that eight genetic variants in *PIP5K1C* were associated with alcohol use disorder in a cohort of African ancestry and that acute alcohol exposure led to up-regulation of PIP5K1C in a mouse model, indicating the potential biological significance of the *PIP5K1C* gene [31], but there was no report about the role of *PIP5K1C* in tumor progression in melanoma. Based on the current results, however, we speculate that *PIP5K1C* is more likely to be a suppressor gene in CM, because a higher mRNA expression of *PIP5K1C* predicted a better survival. Therefore, the molecular mechanisms of genetic variants in *PIP5K1C* underlying the observed association with survival are worthy of further investigation.

*MVB12*B, located on chromosome 9q 33.3, encodes a protein known as multivesicular body subunit 12B, also called a family with sequence similarity 125, member B. The protein product of MVB12B forms a component of the endosomal sorting complex required for transport (ESCRT)-I, a highly conserved complex [32, 33] that is involved in vesicular trafficking (transcytosis); together, these molecules may exert either cancer-promoting or anti-tumoral effects [34, 35] and are also presented either for the establishment or suppression of host immune responses [36, 37]. It is known that MVBs are involved in a variety of diseases, include cancers of the breast, thyroid, ovaries, and colon as well as melanoma [38, 39]. Specifically, it has been reported that the immunological activity of T cells regulated by the phosphorylation of S222 in MVB12B is essential for stimulation of immune STING signaling in recipient cells, resulting in inhibited T-cell proliferation and primed T cells for apoptosis [40].

Recently, a GWAS-based study of intra-ocular pressure (IOP) showed that the SNP rs22868-85 in *MVB12B* was associated with IOP in the TwinsUK cohort, indicating a potential functional role of *MVB12B* in glaucoma [41]. However, no association between *MVB12B* and CM risk or CM survival has been reported. In the present study, we showed that *MVB12B* rs1237-6285 C>T, as a CMSS-associated variant, was associated with reduced *MVB12B* mRNA expression levels in skin fibroblasts, which supports a potential protective role of *MVB12B* in CM. The observation that the rs12376285 T allele may significantly decrease *MVB12B* mRNA expression levels, a possible molecular mechanism underlying the observed association, needs to be validated in additional in-depth mechanistic studies. It has been reported that other micro-environmental factors, such as immune cells, endothelial cells, the extracellular matrix, and soluble molecules, can interact with host fibroblasts to drive tumor progression [42]. Therefore, the role of *MVB12B* in regulating the melanoma microenvironment also warrants additional investigation.

Although no studies on the associations between *PIP5K1C* or *MVB12B* and CMSS have been published, the relevant correlations between the endosome and immunotherapies for CM have been well studied [43]. It is well known that both natural and therapeutically enhanced cytotoxic T lymphocyte (CTL) responses in melanoma patients are of limited efficacy. A recent report demonstrated that the mechanisms underlying the CTL effector-phase fail-

ure in melanoma were related to the endosome system, where human melanoma cells upon conjugation with CTL underwent active late endosome/lysosome trafficking at the lytic synapse, paralleled by cathepsin-mediated perforin degradation and deficient granzyme B penetration [44]. Another recent report showed that a novel peptide antigen-loaded nanoplex vaccine based on the endosome-destabilization inhibited tumor growth and metastasis in murine melanoma models, indicating an immune role of the endosome in the melanoma vaccine [45]. Furthermore, an effective antitumor immune response was induced using a mannose-functionalized endosomolytic nanocomposite(s)-based approach in a C57BL/6 mouse melanoma model, suggesting that prompt endosomal release and escape could be a promising approach to efficient CM immunotherapy [46]. Overall, immune functions, such as antigen presentation, strongly depend on a fully functional endosomal system that delivers exogenous antigens to both MHC class I and MHC class II pathways through cross-presentation of dendritic cells [47, 48]. In addition, human dendritic cells take up the cell-penetrating melanoma antigen peptides through the endosome [49]. Therefore, given the poor prognosis of metastatic CM, genetic variants in endosome-related genes may explain individual variation in response to immunotherapy and thus in prognosis of melanoma patients [50].

Several limitations in the present study should be noted. Compared with the MDACC discovery dataset, the NHS/HPFS validation dataset had fewer participants with fewer variables for further analysis, which could reduce statistical power in validating the effects of other SNPs identified in the discovery. Furthermore, some clinical covariates of the study populations were not available in the NHS/HPFS dataset, further limiting the validation of the findings; however, the consistent survival associations across different datasets in stratification analysis suggest that our results might not be seriously biased by the absence of certain covariates in the replication population. Finally, although several genetic variants in the endosome-related genes backed by *in silico* functional evidence were found to be associated with CMSS, the exact molecular mechanisms through which these SNPs underlie the observed associations remain unclear.

In conclusion, two independent SNPs (i.e., *PIP5K1C* rs11666894 A>C *and MVB12B* rs12376285 C>T) were found to be significantly associated with CMSS in both MDACC discovery and NHS/HPFS replication datasets. The combined analysis revealed that these two SNPs had a significant association with CM survival and that patients with more risk genotypes had a worse prognosis, possibly through the allelic effects on their gene expression. Our findings provide new insights for additional functional studies to further support these genetic variants of the endosome-related pathway genes as new prognostic biomarkers or as clinical decision-making indicators for CM patients and their caregivers, once these findings are validated by additional large patient studies.

Acknowledgements

The authors would like to thank Sen Yang for his technical assistance and all participants and staff members of the Nurses' Health Study and Health Professionals Follow-Up Study for their valuable contributions as well as the following state cancer registries for their support: AL, AZ, AR, CA, CO, CT, DE, FL, GA, ID, IL, IN, IA, KY, LA, ME, MD, MA, MI, NE, NH, NJ, NY, NC, ND, OH, OK, OR, PA, RI, SC, TN, TX, VA, WA, WY. The authors are also grateful for the support of the Channing Division of Network Medicine, Department of Medicine, Brigham and Women's Hospital, home of the NHS. The authors assume full responsibility for analyses and interpretation of these data. We also thank the John Hopkins University Center for Inherited Disease Research for conducting high-throughput genotyping for our study. We also thank all of the investigators and funding agencies that enabled the deposition of data in dbGaP used here (dbGaP Study Accession: phs000187.v1.p1).

This work was supported by NIH/NCI R01 CA100264, 2P50CA093459, R01 CA133996, R01 CA49449, P01 CA87969, UM1 CA186107, U01 CA167552, The University of Texas MD Anderson Cancer Center Various Donors Melanoma and Skin Cancers Priority Program Fund, the Miriam and Jim Mulva Research Fund, the McCarthy Skin Cancer Research Fund, and the Marit Peterson Fund for Melanoma Research. Qingyi Wei was partly supported by start-up funds from the Duke Cancer Institute, Duke University Medical Center,

and also partly by Duke Cancer Institute as part of the P30 Cancer Center Support Grant (Grant ID: NIH CA014236). Guiqing Lu was sponsored by Nanjing Medical Science and Technique Development Foundation (QRX17-100). The content is solely the responsibility of the authors and does not necessarily represent the official views of the NIH/NCI.

Disclosure of conflict of interest

None.

Abbreviations

APCs, antigen-presenting cells; AUC, area under curve; BFDP, Bayesian false-discovery probability; CI, confidence interval; CM, cutaneous melanoma; CMSS, cutaneous melanoma-specific survival; CTLs, cytotoxic T lymphocytes; DCs, dendritic cells; eQTL, expression quantitative trait loci; ESCRT, endosomal sorting complex required for transport; *FAMB25*, family with sequence similarity 125, member B; GSEA, Gene Set Enrichment Analysis; GTEx, Genotype-Tissue Expression; GWAS, genome-wide association study; HPAs, The Human Protein Altas; HR, hazards ratio; HR_{adj}, adjusted hazards ratio; LD, linkage disequilibrium; MDACC, The University of Texas MD Anderson Cancer Center; MHC, major histocompatibility complex; MHC I, MHC class I molecules; MHC II, MHC class II molecules; MVB12B, multivesicular body subunit 12B; NHS/HPFS, the Nurses' Health Study/Health Professionals Follow-up Study; NRGs, number of risk genotypes; PIP2, phosphatidylinositol (4,5)-bisphosphate; PIP5K1C, Phosphatidylinositol-4-phosphate 5-kinase type-1 gamma; ROC, receiver operating characteristics curve; SNP, single-nucleotide polymorphism; TCGA, the Cancer Genome Atlas; TCR, T cell receptor.

Address correspondence to: Dr. Qingyi Wei, Duke Cancer Institute, Duke University Medical Center, 905 South LaSalle Street, Durham, NC 27710, USA. Tel: 919-660-0562; E-mail: qingyi.wei@duke.edu

References

[1] Schadendorf D, van Akkooi ACJ, Berking C, Griewank KG, Gutzmer R, Hauschild A, Stang A, Roesch A and Ugurel S. Melanoma. Lancet 2018; 392: 971-84.

[2] Siegel RL, Miller KD and Jemal A. Cancer statistics, 2019. CA Cancer J Clin 2019; 69: 7-34.

[3] Herzberg B and Fisher DE. Metastatic melanoma and immunotherapy. Clin Immunol 2016; 172: 105-110.

[4] Luke JJ, Flaherty KT, Ribas A and Long GV. Targeted agents and immunotherapies: optimizing outcomes in melanoma. Nat Rev Clin Oncol 2017; 14: 463-82.

[5] Boland GM and Gershenwald JE. Principles of melanoma staging. Cancer Treat Res 2016; 167: 131-48.

[6] Dai W, Liu H, Xu X, Ge J, Luo S, Zhu D, Amos CI, Fang S, Lee JE, Li X, Nan H, Li C and Wei Q. Genetic variants in ELOVL2 and HSD17B12 predict melanoma-specific survival. Int J Cancer 2019; 145: 2619-2628.

[7] Shastry BS. SNPs: impact on gene function and phenotype. Methods Mol Biol 2009; 578: 3-22.

[8] Visscher PM, Wray NR, Zhang Q, Sklar P, McCarthy MI, Brown MA and Yang J. 10 years of GWAS discovery: biology, function, and translation. Am J Hum Genet 2017; 101: 5-22.

[9] Marjoram P, Zubair A and Nuzhdin SV. Post-GWAS: where next? More samples, more SNPs or more biology? Heredity (Edinb) 2014; 112: 79-88.

[10] Gallagher MD and Chen-Plotkin AS. The post-GWAS era: from association to function. Am J Hum Genet 2018; 102: 717-730.

[11] Witte JS. Genome-wide association studies and beyond. Annu Rev Public Health 2010; 31: 9-20 4 p following 20.

[12] Stasyk T and Huber LA. Spatio-temporal parameters of endosomal signaling in cancer: implicationsfor new treatment options. J Cell Biochem 2016; 117: 836-843.

[13] D'Agostino L, Nie Y, Goswami S, Tong K, Yu S, Bandyopadhyay S, Flores J, Zhang X, Balasubramanian I, Joseph I, Sakamori R, Farrell V, Li Q, Yang CS, Gao B, Ferraris RP, Yehia G, Bonder EM, Goldenring JR, Verzi MP, Zhang L, Ip YT and Gao N. Recycling endosomes in mature epithelia restrain tumorigenic signaling. Cancer Res 2019; 79: 4099-4112.

[14] Ploper D and De Robertis EM. The MITF family of transcription factors: role in endolysosomal biogenesis, Wnt signaling, and oncogenesis. Pharmacol Res 2015; 9: 36-43.

[15] Ostalecki C, Lee JH, Dindorf J, Collenburg L, Schierer S, Simon B, Schliep S, Kremmer E, Schuler G and Baur AS. Multiepitope tissue analysis reveals SPPL3-mediated ADAM10 activation as a key step in the transformation of melanocytes. Sci Signal 2017; 10: eaai8288.

[16] Zhao T, Ding X, Yan C and Du H. Endothelial Rab7 GTPase mediates tumor growth and metastasis in lysosomal acid lipase-deficient mice. J Biol Chem 2017; 292: 19198-19208.

[17] Silva P, Mendoza P, Rivas S, Díaz J, Moraga C, Quest AF and Torres VA. Hypoxia promotes Rab5 activation, leading to tumor cell migration, invasion and metastasis. Oncotarget 2016; 7: 29548-62.
[18] Neefjes J, Jongsma MML and Berlin I. Stop or Go? Endosome positioning in the establishment of compartment architecture, dynamics, and function. Trends Cell Biol 2017; 27: 580-594.
[19] Alloatti A, Kotsias F, Pauwels AM, Carpier JM, Jouve M, Timmerman E, Pace L, Vargas P, Maurin M, Gehrmann U, Joannas L, Vivar OI, Lennon-Duménil AM, Savina A, Gevaert K, Beyaert R, Hoffmann E and Amigorena S. Toll-like receptor 4 engagement on dendritic cells restrains phago-lysosome fusion and promotes cross-presentation of antigens. Immunity 2015; 43: 1087-1100.
[20] Miller BC, Sen DR, Al Abosy R, Bi K, Virkud YV, LaFleur MW, Yates KB, Lako A, Felt K, Naik GS, Manos M, Gjini E, Kuchroo JR, Ishizuka JJ, Collier JL, Griffin GK, Maleri S, Comstock DE, Weiss SA, Brown FD, Panda A, Zimmer MD, Manguso RT, Hodi FS, Rodig SJ, Sharpe AH and Haining WN. Subsets of exhausted CD8+ T cells differentially mediate tumor control and respond to checkpoint blockade. Nat Immunol 2019; 20: 326-336.
[21] Amos CI, Wang LE, Lee JE, Gershenwald JE, Chen WV, Fang S, Kosoy R, Zhang M, Qureshi AA, Vattathil S, Schacherer CW, Gardner JM, Wang Y, Bishop DT, Barrett JH; GenoMEL Investigators, MacGregor S, Hayward NK, Martin NG, Duffy DL; Q-Mega Investigators, Mann GJ, Cust A, Hopper J; AMFS Investigators, Brown KM, Grimm EA, Xu Y, Han Y, Jing K, McHugh C, Laurie CC, Doheny KF, Pugh EW, Seldin MF, Han J and Wei Q. Genome-wide association study identifies novel loci predisposing to cutaneous melanoma. Hum Mol Genet 2011; 20: 5012-5023.
[22] Song F, Qureshi AA, Zhang J, Amos CI, Lee JE, Wei Q and Han J. Exonuclease 1 (EXO1) gene variation and melanoma risk. DNA Repair (Amst) 2012; 11: 304-309.
[23] Nader GP, Ezratty EJ and Gundersen GG. FAK, talin and PIPKIγ regulate endocytosed integrin activation to polarize focal adhesion assembly. Nat Cell Biol 2016; 18: 491-503.
[24] Li X, Zhou Q, Sunkara M, Kutys ML, Wu Z, Rychahou P, Morris AJ, Zhu H, Evers BM and Huang C. Ubiquitylation of phosphatidylinositol 4-phosphate 5-kinase type I γ by HECTD1 regulates focal adhesion dynamics and cell migration. J Cell Sci 2013; 126: 2617-2628.
[25] Jafari N, Zheng Q, Li L, Li W, Qi L, Xiao J, Gao T and Huang C. p70S6K1 (S6K1)-mediated phosphorylation regulates phosphatidylinositol 4-phosphate 5-kinase type I γ degradation and cell invasion. J Biol Chem 2016; 291: 25729-25741.
[26] Xu W, Wang P, Petri B, Zhang Y, Tang W, Sun L, Kress H, Mann T, Shi Y, Kubes P and Wu D. Integrin-induced PIP5K1C kinase polarization regulates neutrophil polarization, directionality, and in vivo infiltration. Immunity 2010; 33: 340-50.
[27] van den Bout I and Divecha N. PIP5K-driven PtdIns(4,5)P2 synthesis: regulation and cellular functions. J Cell Sci 2009; 122: 3837-50.
[28] Schill NJ, Hedman AC, Choi S and Anderson RA. Isoform 5 of PIPKIγ regulates the endosomal trafficking and degradation of E-cadherin. J Cell Sci 2014; 127: 2189-203.
[29] Tuosto L, Capuano C, Muscolini M, Santoni A and Galandrini R. The multifaceted role of PIP2 in leukocyte biology. Cell Mol Life Sci 2015; 72: 4461-74.
[30] Van den Bossche J, Malissen B, Mantovani A, De Baetselier P and Van Ginderachter JA. Regulation and function of the E-cadherin/catenin complex in cells of the monocyte-macrophage lineage and DCs. Blood 2012; 19: 1623-33.
[31] Lee JS, Sorcher JL, Rosen AD, Damadzic R, Sun H, Schwandt M, Heilig M, Kelly J, Mauro KL, Luo A, Rosoff D, Muench C, Jung J, Kaminsky ZA and Lohoff FW. Genetic association and expression analyses of the phosphatidylinositol-4-phosphate 5-kinase (PIP5K1C) gene in alcohol use disorder-relevance for pain signaling and alcohol use. Alcohol Clin Exp Res 2018; 42: 1034-1043.
[32] Piper RC and Katzmann DJ. Biogenesis and function of multivesicular bodies. Annu Rev Cell Dev Biol 2007; 23: 519-47.
[33] Tsunematsu T, Yamauchi E, Shibata H, Maki M, Ohta T and Konishi H. Distinct functions of human MVB12A and MVB12B in the ESCRT-I dependent on their posttranslational modifications. Biochem Biophys Res Commun 2010; 399: 232-7.
[34] Tkach M and Théry C. Communication by extracellular vesicles: where we are and where we need to go. Cell 2016; 164: 1226-1232.
[35] Desrochers LM, Antonyak MA and Cerione RA. Extracellular vesicles: satellites of information transfer in cancer and stem cell biology. Dev Cell 2016; 37: 301-309.
[36] Buck AH, Coakley G, Simbari F, McSorley HJ, Quintana JF, Le Bihan T, Kumar S, Abreu-Goodger C, Lear M, Harcus Y, Ceroni A, Babayan SA, Blaxter M, Ivens A and Maizels RM. Exosomes secreted by nematode parasites transfer smallRNAs to mammalian cells and modulate innate immunity. Nat Commun 2014; 5: 5488.

[37] Cwiklinski K, de la Torre-Escudero E, Trelis M, Bernal D, Dufresne PJ, Brennan GP, O'Neill S, Tort J, Paterson S, Marcilla A, Dalton JP and Robinson MW. The extracellular vesicles of the helminth pathogen, fasciola hepatica: biogenesis pathways and cargo molecules involved inparasite pathogenesis. Mol Cell Proteomics 2015; 14: 3258-3273.

[38] Latifkar A, Ling L, Hingorani A, Johansen E, Clement A, Zhang X, Hartman J, Fischbach C, Lin H, Cerione RA and Antonyak MA. Loss of sirtuin 1 alters the secretome of breast cancer cells by impairing lysosomal integrity. Dev Cell 2019; 49: 393-408.

[39] Burgoyne T, Jolly R, Martin-Martin B, Seabra MC, Piccirillo R, Schiaffino MV and Futter CE. Expression of OA1 limits the fusion of a subset of MVBs with lysosomes - a mechanism potentially involved in the initial biogenesis of melanosomes. J Cell Sci 2013; 126: 5143-52.

[40] Nandakumar R, Tschismarov R, Meissner F, Prabakaran T, Krissanaprasit A, Farahani E, Zhang BC, Assil S, Martin A, Bertrams W, Holm CK, Ablasser A, Klause T, Thomsen MK, Schmeck B, Howard KA, Henry T, Gothelf KV, Decker T and Paludan SR. Intracellular bacteria engage a STING-TBK1-MVB12b pathway to enable paracrine cGAS-STING signalling. Nat Microbiol 2019; 4: 701-713.

[41] Nag A, Venturini C, Small KS, Young TL, Viswanathan AC, Mackey DA, Hysi PG and Hammond C. A genome-wide association study of intraocular pressure suggests a novel association in the gene FAM125B in the TwinsUK cohort. Hum Mol Genet 2014; 23: 3343-8.

[42] Flach EH, Rebecca VW, Herlyn M, Smalley KS and Anderson AR. Fibroblasts contribute to melanoma tumor growth and drug resistance. Mol Pharm 2011; 8: 2039-49.

[43] Chaput N, Taïeb J, Schartz NE, André F, Angevin E and Zitvogel L. Exosome-based immunotherapy. Cancer Immunol Immunother 2004; 53: 234-9.

[44] Khazen R, Müller S, Gaudenzio N, Espinosa E, Puissegur MP and Valitutti S. Melanoma cell lysosome secretory burst neutralizes the CTL-mediated cytotoxicity at the lytic synapse. Nat Commun 2016; 7: 10823.

[45] Qiu F, Becker KW, Knight FC, Baljon JJ, Sevimli S, Shae D, Gilchuk P, Joyce S and Wilson JT. Poly (propylacrylic acid)-peptide nanoplexes as a platform for enhancing the immunogenicity of neoantigen cancer vaccines. Biomaterials 2018; 182: 82-9.

[46] Sharma R and Vyas SP. Mannose functionalized plain and endosomolytic nanocomposite(s)-based approach for the induction of effective antitumor immune response in C57BL/6 mice melanoma model. Drug Dev Ind Pharm 2019; 45: 1089-1100.

[47] Shin JS, Ebersold M, Pypaert M, Delamarre L, Hartley A and Mellman I. Surface expression of MHC class II in dendritic cells is controlled by regulated ubiquitination. Nature 2006; 444: 115-18.

[48] Mellman I and Steinman RM. Dendritic cells: specialized and regulated antigen processing machines. Cell 2001; 106: 255-8.

[49] Li H, van der Leun AM, Yofe I, Lubling Y, Gelbard-Solodkin D, van Akkooi ACJ, van den Braber M, Rozeman EA, Haanen JBAG, Blank CU, Horlings HM, David E, Baran Y, Bercovich A, Lifshitz A, Schumacher TN, Tanay A and Amit I. Dysfunctional CD8 T cells form a proliferative, dynamically regulated compartment within human melanoma. Cell 2019; 176: 775-789.

[50] Weiss SA, Wolchok JD and Sznol M. Immunotherapy of melanoma: facts and hopes. Clin Cancer Res 2019; 25: 5191-5201.

Supplementary Methods

SNP genotyping

In the discovery MDACC dataset, genomic DNA was extracted from the whole blood samples from cutaneous melanoma (CM) patients and genotyped by using the Illumina HumanOmni-Quad_v1_0_B array. The genotyping data are available at the National Center for Biotechnology Information Database of Genotypes and Phenotypes (dbGaP Study Accession: phs000187.v1.p1). We performed genome-wide imputation based on the 1000 Genomes Project, phase I v2 CEU, utilizing the MACH software (March 2010 release). Following strict criteria (with an imputation info score ≥0.8, a genotyping rate ≥95%, a minor allelic frequency ≥5%, and Hardy-Weinberg equilibrium $\geq 1\times10^{-5}$), we extracted both typed and imputed SNPs within ± 2 kilobase flanking regions of the endosome-related pathway genes from the MDACC CM GWAS dataset. For the NHS/HPFS validation dataset, genotyping of DNA samples was performed with the HumanHap610 array, Affymetrix 6.0 array, and Illumina HumanHap550 array. We performed additional imputation depending on haplotype information and genotyped SNPs from phase II HapMap CEU data by applying the MACH program (March 2012 release). We extracted the genotyping data from the NHS/HPFS CM GWAS datasets, following the same quality control criteria for those from the MDACC CM GWAS dataset.

Statistical methods

For the present study, we defined CMSS as the period from the date of diagnosis of CM to the date of death from CM. CM patients known to be alive were censored at the time of the last contact. In the MDACC genotyping dataset, we first assessed the associations between all available SNPs in 228 endosome-related pathway genes and CMSS in a single-locus Cox proportional hazards regression analysis using the GenABEL package of R software. Then, multivariate Cox regression analyses were performed with adjustment for available covariates in the MDACC dataset (including age, sex, Breslow thickness, mitotic rate, distant/regional metastasis and ulceration); however, in the validation NHS/HPFS genotyping dataset, the only covariates available for adjustment were age and sex. Because of a high level of linkage disequilibrium (LD) among imputed SNPs, we used Bayesian false discovery probability (BFDP) with a cutoff value of 0.80 for multiple testing correction to lower the probability of potentially false positive results. In addition, we assigned a prior probability of 0.10 and an upper boundary hazards ratio (HR) of 3.0 for an association with variant genotypes or minor alleles of the SNPs with $P<0.05$. Next, we employed a multivariate stepwise Cox regression model to identify independent tagging SNPs in the MDACC dataset that had more covariate information. After that, we performed a meta-analysis to combine the identified SNPs from the MDACC dataset with that in the NHS/HPFS dataset using PLINK 1.90 with the Cochran's Q statistics and I^2. Because there was no significant heterogeneity between the MDACC dataset and the NHS/HPFS dataset (Q test $P>0.1$, $I^2<25.0\%$), we performed the meta-analysis with a fixed-effects model.

We subsequently evaluated cumulative effects of all the identified SNPs via Kaplan-Meier (KM) survival curves, showing CM survival probability associated with the number of the combined alleles. We also calculated the receiver operating characteristic (ROC) curve and time-dependent area under the curve (AUC) by using the timeROC package of R software (version 3.5.0) to predict effects of both clinical and genetic variables on CMSS. For stratified analyses by subgroups, we calculated inter-study heterogeneity and evaluated possible interaction. To evaluate genotype-phenotype correlations between genotypes of all the identified SNPs and the mRNA expression of their genes, we performed expression quantitative trait loci (eQTL) analyses with a linear regression model using the data from the 373 European descendants included in the 1000 Genomes Project and the genotype-tissue expression (GTEx) project (http://www.gtexportal.org/home) using R software (version 3.5.0). All statistical analyses were performed with SAS software (version 9.4; SAS Institute, Cary, NC), unless specified otherwise.

Table S1. List of 228 selected genes in the endosome-related pathway

Dataset	Name of pathway	Number of genes
GO	VESICLE_MEDIATED_TRANSPORT_BETWEEN_ENDOSOMAL_COMPARTMENTS	41
GO	REGULATION_OF_EARLY_ENDOSOME_TO_LATE_ENDOSOME_TRANSPORT	17
GO	MULTIVESICULAR_BODY_ORGANIZATION	31
GO	ENDOCYTOSIS	181
KEGG	SYNTHESIS_OF_PIPS_AT_THE_EARLY_ENDOSOME_MEMBRANE	16
REACTOME	SYNTHESIS_OF_PIPS_AT_THE_LATE_ENDOSOME_MEMBRANE	11
Total	*CHMP1A, CHMP1B, CHMP2A, CHMP2B, CHMP3, CHMP4A, CHMP4B, CHMP4C, CHMP5, CHMP6, CHMP7, HGS, IST1, MVB12A, PDCD6IP, RAB11A, RAB27A, SNF8, STAM, STAM2, TSG101, VPS25, VPS28, VPS36, VPS37A, VPS37B, VPS37C, VPS37D, VPS4A, VPS4B, VTA1, DAB2, DNAJC13, EZR, MAP2K1, MAP2K2, MAPK1, MAPK3, MTMR2, PTPN23, RAB21, RDX, SNX3, SRC, VPS11, AKTIP, ANKRD27, BECN1, CORO1A, EEA1, EMP2, FAM160A2, HOOK1, HOOK2, HOOK3, KIF16B, LMTK2, MYO1D, PIK3C3, RAB5A, RAB7A, RILP, SNX16, SORL1, STX8, WASH3P, WDR81, WDR91, ACAP1, ACAP2, ACAP3, ADRB1, ADRB2, ADRB3, AGAP1, AGAP2, AP2A1, AP2A2, AP2B1, AP2M1, AP2S1, ARAP1, ARAP2, ARAP3, ARF6, ARFGAP1, ARFGAP2, ARFGAP3, ARRB1, ARRB2, ASAP1, ASAP2, ASAP3, CBL, CBLB, CBLC, CCR5, CDC42, CLTA, CLTB, CLTC, CLTCL1, CSF1R, CXCR1, CXCR2, CXCR4, DNAJC6, DNM1, DNM1L, DNM2, DNM3, EGF, EGFR, EHD1, EHD2, EHD3, EHD4, EPN1, EPN2, EPN3, EPS15, ERBB3, ERBB4, F2R, FGFR2, FGFR3, FGFR4, FLT1, GIT1, GIT2, GRK1, ADRBK1, ADRBK2, GRK4, GRK5, GRK6, GRK7, HLA-A, HLA-B, HLA-C, HLA-E, HLA-F, HLA-G, HRAS, HSPA1A, HSPA1B, HSPA1L, HSPA2, HSPA6, HSPA8, IGF1R, IL2RA, IL2RB, IQSEC1, IQSEC3, ITCH, KDR, KIT, LDLR, LDLRAP1, MDM2, MET, MVB12B, NEDD4, NEDD4L, NTRK1, PARD3, PARD6A, PARD6B, PARD6G, PDGFRA, PIKFYVE, PIP4K2B, PIP5K1A, PIP5K1B, PIP5K1C, PLD1, PLD2, PRKCI, PRKCZ, PSD, PSD2, PSD3, PSD4, RAB11B, RAB11FIP1, RAB11FIP2, RAB11FIP3, RAB11FIP4, RAB11FIP5, RAB22A, RAB31, RAB4A, RAB5C, RABEP1, ZFYVE20, RET, RNF41, RUFY1, SH3GL1, SH3GL2, SH3GL3, SH3GLB1, SH3GLB2, SMAP1, SMAP2, SMURF1, SMURF2, STAMBP, TFRC, TRAF6, USP8, VPS45, WWP1, FIG4, INPP4A, INPP4B, INPP5F, MTMR10, MTMR12, MTMR4, PI4K2A, PI4K2B, PIK3C2A, PIK3R4, VAC14, MTMR7, MTMR9* (after removing the duplicated 62 genes, six genes in X chromosome, one pseudogene)	228

Keyword: endosome phase/phases; Organism: Homo sapiens; Website: http://software.broadinstitute.org/gsea/msigdb/search.jsp.

Table S2. Distributions of the characteristics of CM patients in the MDACC and Harvard genotyping datasets

Parameter		Frequency		MFT	HR (95% CI)[a]	*P*[a]
		Patient	Death (%)			
MDACC		858	95 (11.1)	81.1		
Age (years)	≤50	371	31 (8.4)	85.8	1.00	
	>50	487	64 (13.1)	78.1	1.69 (1.10-2.59)	0.017
Sex	Female	362	26 (7.2)	85.9	1.00	
	Male	496	69 (13.9)	77.8	2.07 (1.32-3.25)	0.002
Regional/distant metastasis	No	709	51 (7.2)	82.7	1.00	
	Yes	149	44 (29.5)	69.4	4.78 (3.19-7.15)	<0.001
Breslow thickness (mm)	≤1	347	7 (2.0)	85.0	1.00	
	>1	511	88 (17.2)	78.1	9.17 (4.25-19.80)	<0.001
Ulceration	No	681	48 (7.1)	84.0	1.00	
	Yes	155	43 (27.7)	64.3	4.91 (3.29-7.42)	<0.001
	Missing	22				
Mitotic rate (/mm^2)	≤1	275	9 (3.3)	82.2	1.00	
	>1	583	86 (14.8)	80.1	4.67 (2.35-9.29)	<0.001
Harvard		409	48 (11.7)	179.0		
Age (years)	≤50	72	3 (4.2)	352.5	1.00	
	>50	337	45 (13.4)	167.0	4.04 (1.25-13.06)	0.020
Sex	Female	271	31 (11.4)	198.0	1.00	
	Male	138	17 (12.3)	155.5	1.16 (0.64-2.10)	0.622

Abbreviations: CM, cutaneous melanoma; MDACC, The University of Texas MD Anderson Cancer Center; MFT, median follow-up time (months); HR, hazards ratio; CI, confidence interval. [a]Univariate Cox proportional hazards regression analysis.

Table S3. Functional prediction of 38 validated SNPs in high linkage disequilibrium (LD) ($r^2 \geq 0.8$) in endosome-related pathway genes

Chr	Variant	Ref	Alt	Enhancer histone marks	DNAse	Motifs changed	GRASP QTL hits	Selected eQTL hits	GENCODE genes	dbSNP
2	rs72991127	G	C			6 altered motifs		5 hits	*AGAP1*	intronic
3	rs77278014	A	C	17 tissues	5 tissues	BDP1, Hsf			*IQSEC1*	intronic
9	rs7023712	G	A	ESDR, BLD		Pou2f2		2 hits	*FAM125B*	intronic
9	rs7039136	T	G			Ncx, Nkx2, Nkx3		1 hit	*FAM125B*	intronic
9	rs10987304	G	A			GR, Pbx3			*FAM125B*	intronic
9	rs4260977	T	C	BLD, SKIN, BRST		BCL			*FAM125B*	intronic
9	rs7027798	C	G	SKIN		37 altered motifs			*FAM125B*	intronic
9	rs758969	A	G	SKIN		5 altered motifs			*FAM125B*	intronic
9	rs758968	A	G						*FAM125B*	intronic
9	rs62578063	C	T	BLD		AP-1, TFII-I			*FAM125B*	intronic
9	rs1610019	G	A	BLD				1 hit	*FAM125B*	intronic
9	rs3915928	A	C	BLD					*FAM125B*	intronic
9	rs4373626	C	G	BLD		4 altered motifs		2 hits	*FAM125B*	intronic
9	rs10987311	C	T		ESDR	13 altered motifs			FAM125B	
9	rs10987312	C	T		4 tissues	4 altered motifs		2 hits	*FAM125B*	
9	rs10987313	G	A					2 hits	*FAM125B*	
9	rs10987314	G	A		BLD	4 altered motifs		2 hits	*FAM125B*	
9	rs74055579	A	G	11 tissues	9 tissues	HDAC2, HNF4			*FAM125B*	intronic
19	rs7247419	G	A	SKIN	7 tissues			7 hits	*PIP5K1C*	intronic
9	rs1548788	G		BLD, BRN, MUS	IPSC	Hsf, Spz1		2 hits	*FAM125B*	intronic
9	rs3928392	A	G	BLD, BRN, MUS	MUS	8 altered motifs			*FAM125B*	intronic
9	rs28569307	C	A	4 tissues		6 altered motifs			*FAM125B*	intronic
9	rs57124607	T	C	8 tissues	6 tissues	PU.1, TCF12, TR4	1 hit		*FAM125B*	intronic
9	rs12004771	G	A	8 tissues	6 tissues	8 altered motifs		2 hits	*FAM125B*	intronic
9	rs56287675	C	G	8 tissues	11 tissues	BCL, Spz1			*FAM125B*	intronic
9	rs28376322	T	C	14 tissues	10 tissues	4 altered motifs			*FAM125B*	intronic
9	rs62578078	C	T	19 tissues	10 tissues				*FAM125B*	intronic
9	rs73670227	A	C	19 tissues	12 tissues	15 altered motifs			*FAM125B*	intronic
9	rs10121265	G	A	18 tissues		5 altered motifs			*FAM125B*	intronic
9	rs12380523	T	C	9 tissues					*FAM125B*	intronic
9	rs28495310	T	C	9 tissues	BLD, MUS	Myc, NRSF, Sin3Ak-20		1 hit	*FAM125B*	intronic
9	rs62578079	C	G	10 tissues	MUS, MUS, SKIN	5 altered motifs		1 hit	*FAM125B*	3'-UTR
9	rs3814128	C	A	10 tissues	4 tissues	22 altered motifs			*FAM125B*	3'-UTR
9	rs3814126	G	C	10 tissues	9 tissues	ZEB1		2 hits	*FAM125B*	3'-UTR
9	rs3739566	G	A	6 tissues		11 altered motifs			*FAM125B*	3'-UTR
9	rs3814124	A	G	ESDR, BRN, PANC	4 altered motifs	11 altered motifs			*FAM125B*	3'-UTR
9	rs12376285	C	T	4 tissues	IPSC			2 hits	*FAM125B*	
19	rs11666894	A	C			4 altered motifs		1 hit	*PIP5K1C*	intronic

Abbreviations: SNP, single-nucleotide polymorphism; Chr, chromosome; dbSNP func annot, dbSNP function annotation; *AGAP1,* ArfGAP With GTPase Domain, Ankyrin Repeat and PH Domain 1; IQSEC1, IQ motif and SEC7 domain-containing protein 1; FAM125B (alias for MVB12B gene), Family With Sequence Similarity 125, Member B; IQSEC3, IQ motif and SEC7 domain-containing protein 3; PIP5K1C, phosphatidylinositol-4-phosphate 5-kinase type 1 gamma. HaploReg v4.1 (http://archive.broadinstitute.org/mammals/haploreg/haploreg.php).

Table S4. Meta-analysis of 38 validated SNPs in endosome-related pathway genes using two independently published melanoma GWAS datasets

SNP	Allele[1]	Gene	Discovery-MDACC (n=858)				Replication-NHS/HPFS (n=409)				Combined-Meta-analysis (n=1267)			
			EAF	HR (95% CI)	P^2	BFDP	EAF	HR (95% CI)	P^3	BFDP	P_{het}	I^2	HR (95% CI)	P^4
rs72991127$	G>C	*AGAP1*	0.24	1.46 (1.05-2.04)	0.025	0.738	0.27	1.60 (1.03-2.48)	0.036	0.777	0.744	0	1.51 (1.16-1.97)	0.002
rs77278014$	A>C	*IQSEC1*	0.06	1.74 (1.09-2.78)	0.020	0.718	0.09	2.13 (1.25-3.62)	0.006	0.558	0.576	0	1.90 (1.34-2.70)	3.00×10^{-4}
rs7023712$	G>A	*MVB12B*	0.17	1.62 (1.11-2.39)	0.013	0.660	0.20	1.72 (1.12-2.64)	0.012	0.649	0.838	0	1.66 (1.25-2.21)	4.70×10^{-4}
rs7039136$	T>G	*MVB12B*	0.18	1.62 (1.11-2.38)	0.014	0.648	0.20	1.67 (1.08-2.58)	0.021	0.714	0.918	0	1.64 (1.23-2.19)	0.001
rs10987304$	G>A	*MVB12B*	0.17	1.57 (1.07-2.31)	0.021	0.715	0.20	1.74 (1.13-2.67)	0.012	0.289	0.727	0	1.64 (1.23-2.19)	0.001
rs4260977$	T>C	*MVB12B*	0.17	1.57 (1.07-2.31)	0.021	0.715	0.20	1.74 (1.13-2.67)	0.012	0.626	0.727	0	1.64 (1.23-2.19)	0.001
rs7027798$	C>G	*MVB12B*	0.17	1.56 (1.07-2.29)	0.022	0.721	0.20	1.80(1.17-2.76)	0.005	0.552	0.626	0	1.66 (1.25-2.21)	$4.87\text{x}10^{-4}$
rs758969$	A>G	*MVB12B*	0.17	1.57 (1.07-2.31)	0.021	0.715	0.20	1.70 (1.10-2.63)	0.018	0.688	0.789	0	1.63 (1.22-2.17)	0.001
rs758968$	A>G	*MVB12B*	0.17	1.57 (1.07-2.30)	0.022	0.705	0.20	1.74 (1.13-2.67)	0.012	0.626	0.727	0	1.64 (1.23-2.19)	0.001
rs62578063$	C>T	*MVB12B*	0.17	1.57 (1.07-2.31)	0.021	0.715	0.20	1.74 (1.13-2.67)	0.012	0.626	0.727	0	1.64 (1.23-2.19)	0.001
rs1610019$	G>A	*MVB12B*	0.17	1.57 (1.07-2.31)	0.021	0.715	0.20	1.76 (1.14-2.73)	0.011	0.634	0.700	0	1.65 (1.24-2.20)	0.001
rs3915928$	A>C	*MVB12B*	0.17	1.57 (1.07-2.31)	0.021	0.715	0.20	1.62 (1.05-2.49)	0.029	0.748	0.915	0	1.59 (1.20-2.12)	0.001
rs4373626$	C>G	*MVB12B*	0.17	1.57 (1.07-2.31)	0.021	0.715	0.20	1.76 (1.14-2.73)	0.011	0.634	0.700	0	1.65 (1.24-2.20)	0.001
rs10987311$	C>T	*MVB12B*	0.17	1.75 (1.19-2.56)	0.004	0.434	0.20	1.71 (1.10-2.66)	0.017	0.691	0.938	0	1.73 (1.30-2.31)	1.87×10^{-4}
rs10987312$	C>T	*MVB12B*	0.17	1.75 (1.19-2.56)	0.004	0.434	0.20	1.71 (1.10-2.66)	0.017	0.691	0.938	0	1.73 (1.30-2.31)	1.87×10^{-4}
rs10987313#	G>A	*MVB12B*	0.17	1.75 (1.19-2.56)	0.004	0.434	0.20	1.71 (1.10-2.66)	0.017	0.691	0.938	0	1.73 (1.30-2.31)	1.87×10^{-4}
rs10987314$	G>A	*MVB12B*	0.17	1.75 (1.19-2.56)	0.004	0.434	0.20	1.71(1.10-2.66)	0.017	0.691	0.938	0	1.73 (1.30-2.31)	1.87×10^{-4}
rs74055579$	A>G	*IQSEC3*	0.09	1.59 (1.02-2.48)	0.039	0.791	0.10	1.90 (1.08-3.33)	0.026	0.758	0.626	0	1.70 (1.20-2.41)	0.003
rs7247419$	A>G	PIP5K1C	0.46	0.72 (0.53-0.98)	0.037	0.782	0.42	0.59 (0.37-0.92)	0.020	0.710	0.475	0	0.68 (0.52-0.87)	0.003
rs1548788#	G>A	MVB12B	0.17	1.57 (1.07-2.31)	0.021	0.715	0.20	1.76 (1.14-2.73)	0.011	0.634	0.700	0	1.65 (1.24-2.20)	0.001
rs3928392$	A>G	MVB12B	0.17	1.57 (1.07-2.31)	0.021	0.715	0.20	1.76 (1.14-2.73)	0.011	0.634	0.700	0	1.65 (1.24-2.20)	0.001
rs28569307$	C>A	MVB12B	0.17	1.57 (1.07-2.31)	0.021	0.715	0.20	1.76 (1.14-2.73)	0.011	0.634	0.700	0	1.65 (1.24-2.20)	0.001
rs57124607$	T>C	MVB12B	0.17	1.57 (1.07-2.31)	0.021	0.715	0.20	1.75 (1.13-2.71)	0.011	0.640	0.715	0	1.65 (1.23-2.20)	0.001
rs12004771$	G>A	MVB12B	0.17	1.57 (1.07-2.31)	0.021	0.715	0.20	1.75 (1.13-2.71)	0.011	0.640	0.715	0	1.65 (1.23-2.20)	0.001
rs56287675$	C>G	MVB12B	0.17	1.58 (1.08-2.32)	0.019	0.698	0.20	1.68 (1.09-2.61)	0.020	0.716	0.837	0	1.62 (1.22-2.17)	0.001
rs28376322$	T>C	MVB12B	0.18	1.51 (1.04-2.21)	0.032	0.769	0.21	1.68 (1.08-2.62)	0.022	0.723	0.720	0	1.58 (1.18-2.11)	0.002
rs62578078$	C>T	MVB12B	0.18	1.51 (1.04-2.21)	0.031	0.769	0.21	1.68 (1.08-2.62)	0.022	0.723	0.720	0	1.58 (1.18-2.11)	0.002
rs73670227$	A>T	MVB12B	0.18	1.51 (1.04-2.21)	0.031	0.769	0.21	1.68 (1.08-2.62)	0.022	0.723	0.720	0	1.58 (1.18-2.11)	0.002
rs10121265$	G>A	MVB12B	0.18	1.51 (1.04-2.21)	0.031	0.769	0.21	1.68 (1.08-2.62)	0.022	0.723	0.720	0	1.58 (1.18-2.11)	0.002
rs12380523$	T>C	MVB12B	0.18	1.51 (1.04-2.21)	0.031	0.769	0.21	1.68 (1.08-2.62)	0.022	0.723	0.720	0	1.58 (1.18-2.11)	0.002
rs28495310$	T>C	MVB12B	0.18	1.51 (1.04-2.21)	0.031	0.769	0.21	1.68 (1.08-2.62)	0.022	0.723	0.720	0	1.58 (1.18-2.11)	0.002
rs62578079$	C>G	MVB12B	0.18	1.51 (1.04-2.21)	0.031	0.769	0.21	1.70 (1.10-2.65)	0.018	0.704	0.690	0	1.59 (1.19-2.11)	0.002

rs3814128[$]	C>A	MVB12B	0.17	1.52 (1.04-2.22)	0.029	0.755	0.21	1.68 (1.07-2.63)	0.024	0.730	0.739	0	1.58 (1.19-2.12)	0.002
rs3814126[#]	G>C	MVB12B	0.17	1.52 (1.04-2.22)	0.029	0.755	0.20	1.63 (1.04-2.55)	0.033	0.767	0.815	0	1.56 (1.17-2.09)	0.002
rs3739566[$]	G>A	MVB12B	0.17	1.64 (1.12-2.41)	0.011	0.621	0.19	1.63 (1.05-2.54)	0.030	0.762	0.984	0	1.64 (1.23-2.18)	0.001
rs3814124[$]	A>G	MVB12B	0.17	1.63 (1.12-2.39)	0.011	0.628	0.19	1.64 (1.05-2.56)	0.029	0.757	0.984	0	1.63 (1.22-2.18)	0.001
rs12376285[$]	C>T	MVM12B	0.17	1.75 (1.19-2.56)	0.004	0.434	0.19	1.71 (1.10-2.66)	0.017	0.691	0.938	0	1.73 (1.30-2.31)	1.87×10^{-4}
rs11666894[$]	A>C	PIP5K1C	0.46	1.40 (1.03-1.91)	0.033	0.771	0.49	1.61 (1.08-2.44)	0.022	0.709	0.593	0	1.47 (1.15-1.89)	0.002

[1]Reference allele/effect allele; [2]Adjusted for age, sex, Breslow thickness,distant/regional metastasis, ulceration and mitotic rate in the additive model; [3]Adjusted for age and sex in the additive model; [4]Meta-analysis in the fix-effect model; [$]Imputed SNP; [#]Genotyped SNP. Abbreviations: SNP, single-nucleotide polymorphism; GWAS, genome-wide association study; MDACC, MD Anderson Cancer Center; EAF, effect allele frequency; HR, hazards ratio; CI, confidence interval; BFDP, Bayesian false-discovery probability; P_{het}, *P* value for heterogeneity by Cochrane's Q test; *AGAP1*, ArfGAP With GTPase Domain, Ankyrin Repeat And PH Domain 1; *IQSEC1*, IQ motif and SEC7 domain-containing protein 1; *MVB12B*, multivesicular body subunit 12B; *IQSEC3*, IQ motif and SEC7 domain-containing protein 3; *PIP5K1C*, phosphatidylinositol-4-phosphate 5-kinase type 1 gamma.

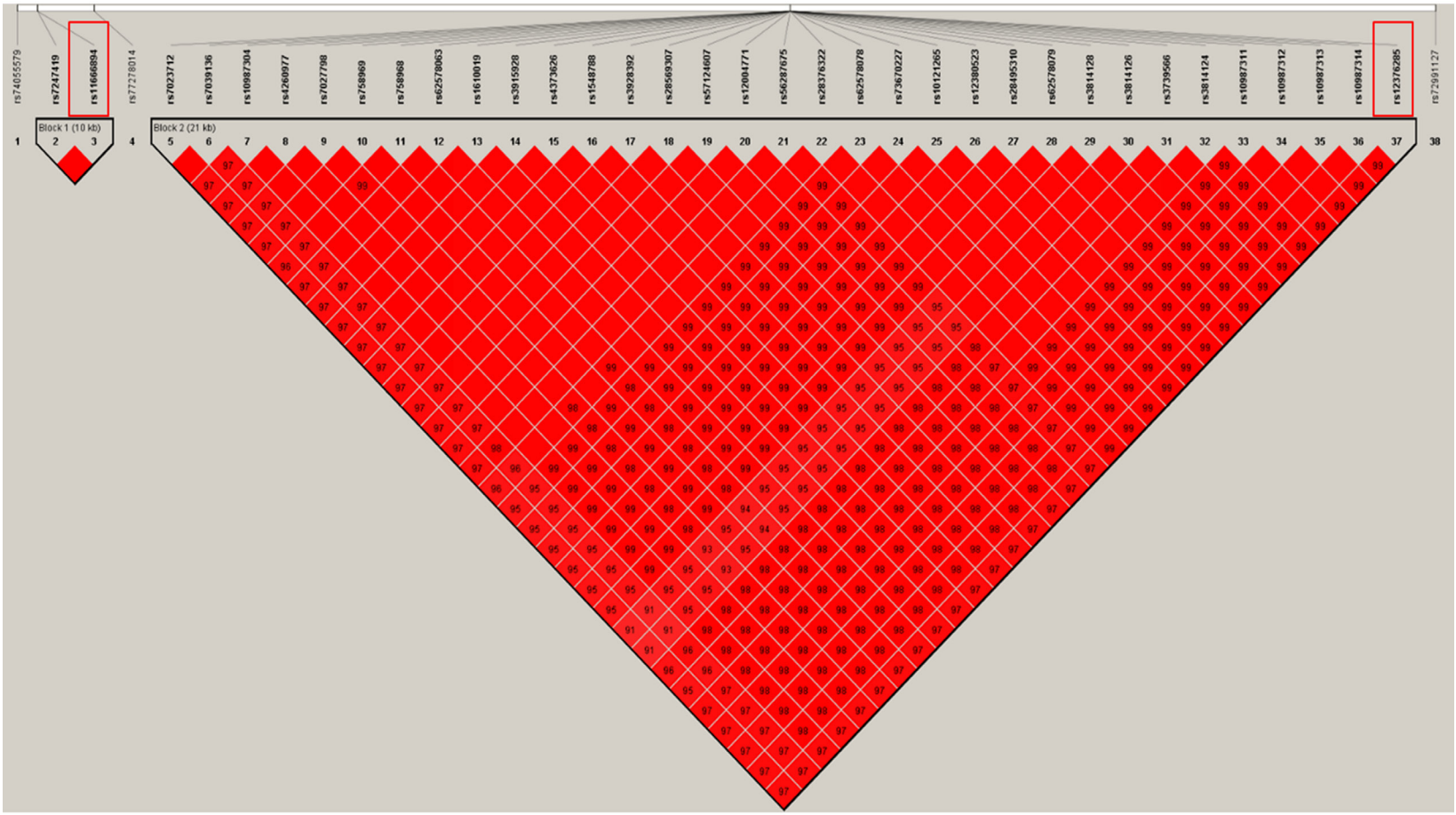

Figure S1. LD plots of 38 SNPs in five genes.

A

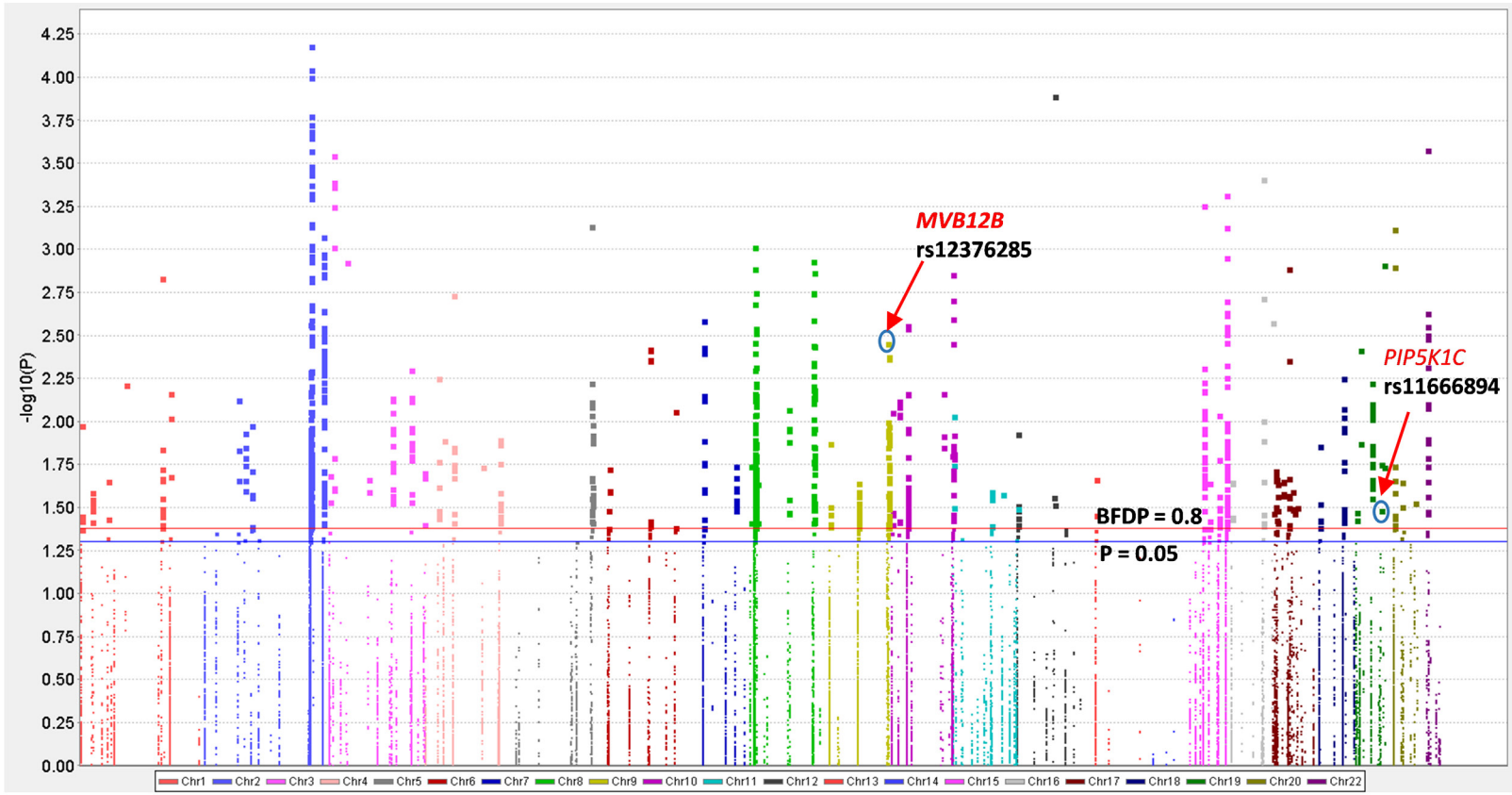
-log10(P)
4.25
4.00
3.75
3.50
3.25
3.00
2.75
2.50
2.25
2.00
1.75
1.50
1.25
1.00
0.75
0.50
0.25
0.00
MVB12B
rs12376285
PIP5K1C
rs11666894
BFDP = 0.8
P = 0.05
Chr1 Chr2 Chr3 Chr4 Chr5 Chr6 Chr7 Chr8 Chr9 Chr10 Chr11 Chr12 Chr13 Chr14 Chr15 Chr16 Chr17 Chr18 Chr19 Chr20 Chr22

B

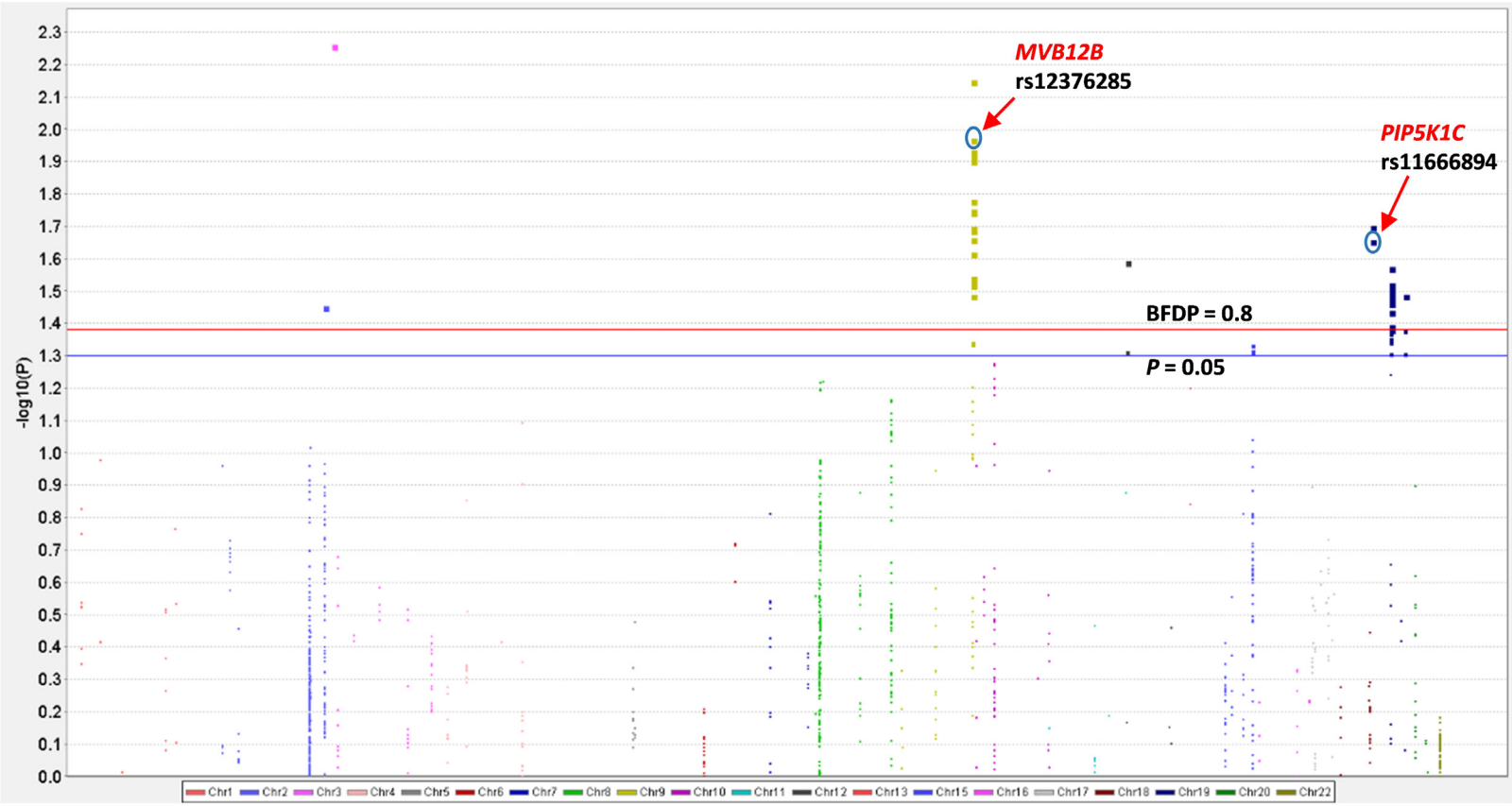

Figure S2. Manhattan plot. A. Manhattan plot for 36,068 SNPs in the MDACC study. B. Manhattan plot for 1925 SNPs in the NHS/HPFS study. The blue horizontal line indicates *P* value equal to 0.05 and the red horizontal line represents BFDP value equal to 0.8. Abbreviations: SNP, single-nucleotide polymorphism; MDACC, the University of Texas MD Anderson Cancer Center; NHS/HPFS, the Nurses' Health Study/Health Professionals Follow-up Study; BFDP, Bayesian false-discovery probability.

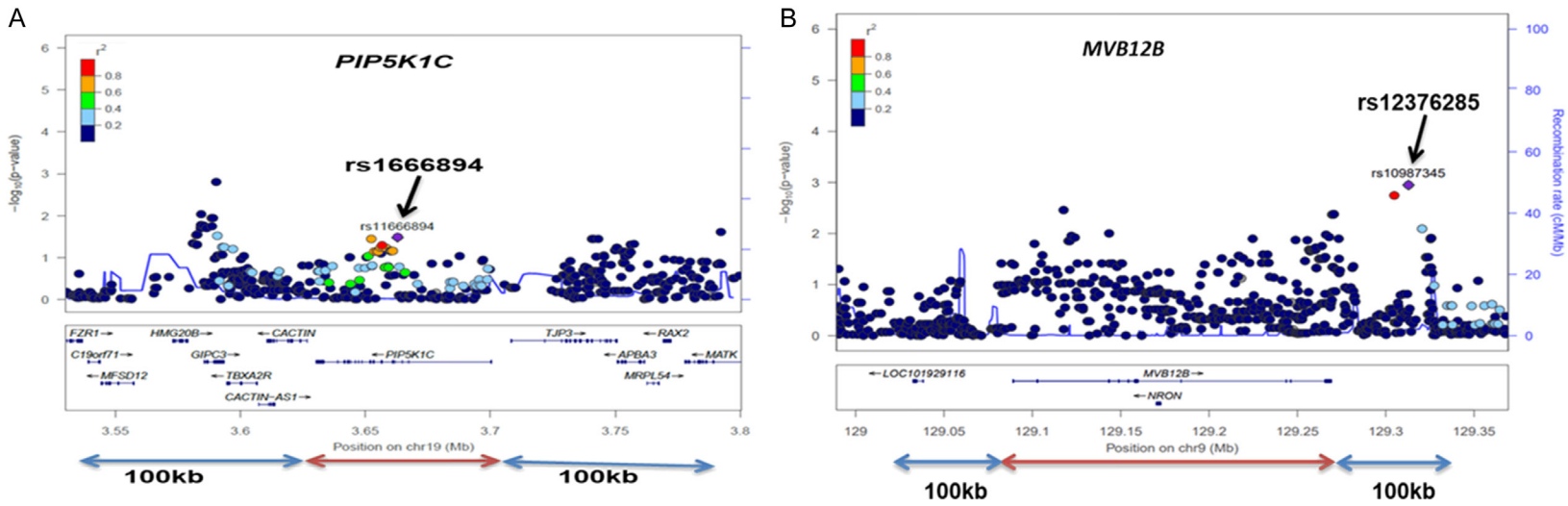

Figure S3. Regional association plots for *PIP5K1C* rs11666894 and *MVB12B* rs12376285. Regional association plots contained 100 kb up and downstream of the gene regions of *PIP5K1C* (A) and *MVB12B* (B).

Table S5. Stratified Cox analysis for risk genotypes of the significant SNPs identified in the MDACC and NHS/HPFS genotyping datasets

Characteristics	0-1 risk genotype[1]		2 risk genotypes[1]		Univariate analysis		Multivariate analysis[2]		Interaction[3]
	All	Death (%)	All	Death (%)	HR (95% CI)	P	HR (95% CI)	P	
MDACC									
Age (years)									
≤60	466	41 (8.80)	128	13 (10.16)	1.16 (0.62-2.16)	0.643	1.42 (0.75-2.69)	0.280	
>60	206	29 (14.08)	58	12 (20.69)	1.52 (0.77-2.97)	0.226	2.18 (1.09-4.39)	0.029	0.237
Sex									
Male	396	52 (13.13)	100	17 (17.00)	1.31 (0.76-2.26)	0.336	1.77 (1.01-3.09)	0.046	
Female	276	180 (6.52)	86	8 (9.30)	1.50 (0.65-3.44)	0.344	1.69 (0.73-3.95)	0.223	0.911
Regional/distant metastasis									
No	550	32 (5.82)	159	19 (11.95)	2.20 (1.24-3.87)	0.007	3.20 (1.76-5.81)	1E-04	
Yes	122	38 (31.15)	27	6 (22.22)	0.61 (0.25-1.45)	0.259	0.73 (0.30-1.74)	0.475	0.010
Breslow thickness (mm)									
≤1	268	5 (1.87)	79	2 (2.53)	1.48 (0.29-7.64)	0.638	1.86 (0.28-12.23)	0.520	
>1	404	65 (16.09)	107	23 (21.50)	1.33 (0.83-2.14)	0.236	1.70 (1.05-2.75)	0.032	0.450
Ulceration									
No	531	33 (6.21)	150	15 (10.00)	1.65 (0.89-3.03)	0.110	2.04 (1.09-3.79)	0.025	
Yes	124	33 (26.61)	31	10 (32.26)	1.27 (0.63-2.58)	0.505	1.40 (0.69-2.86)	0.352	0.407
Missing	22								
Mitotic rate (mm^2)									
≤1	212	8 (3.77)	66	1 (1.59)	0.42 (0.05-3.32)	0.408	0.46 (0.05-4.35)	0.495	
>1	460	62 (13.48)	123	24 (19.51)	1.489 (0.93-2.39)	0.098	1.86 (1.15-3.00)	0.011	0.256
NHS/HPFS									
Age (years)									
≤60	162	13 (8.02)	53	8 (15.09)	1.94 (0.80-4.68)	0.140	1.91 (0.79-4.62)	0.150	
>60	141	12 (8.51)	53	15 (28.30)	3.94 (1.84-8.44)	4E-04	4.05 (1.89-8.69)	3E-04	0.712
Sex									
Male	100	11 (11.00)	38	6 (15.79)	1.43 (0.53-3.87)	0.482	1.37 (0.50-3.71)	0.541	
Female	203	14 (6.90)	68	17 (25.00)	4.15 (2.04-8.42)	<0.001	3.94 (1.94-8.02)	1E-04	0.084

[1]Risk genotypes included *PIP5K1C* rs11666894 AC+CC and *MVB12B* rs12376285 CT+TT; [2]Adjusted for age, sex, Breslow thickness, distant/regional metastasis, ulceration and mitotic rate in Cox models of SNPs and CMSS in the MDACC dataset and adjusted for age and sex only in the NHS/HPFS dataset; [3]Interaction: the interaction between the risk genotypes and each clinical variable. Abbreviations: SNP, single-nucleotide polymorphism; MDACC, The University of Texas MD Anderson Cancer Center; NHS/HPFS, the Nurses' Health Study/Health Professionals Follow-up Study; HR, hazards ratio; CI, confidence interval; *PIP5K1C*, phosphatidylinositol-4-phosphate 5-kinase type 1 gamma; *MVB12*B, multivesicular body subunit 12B.

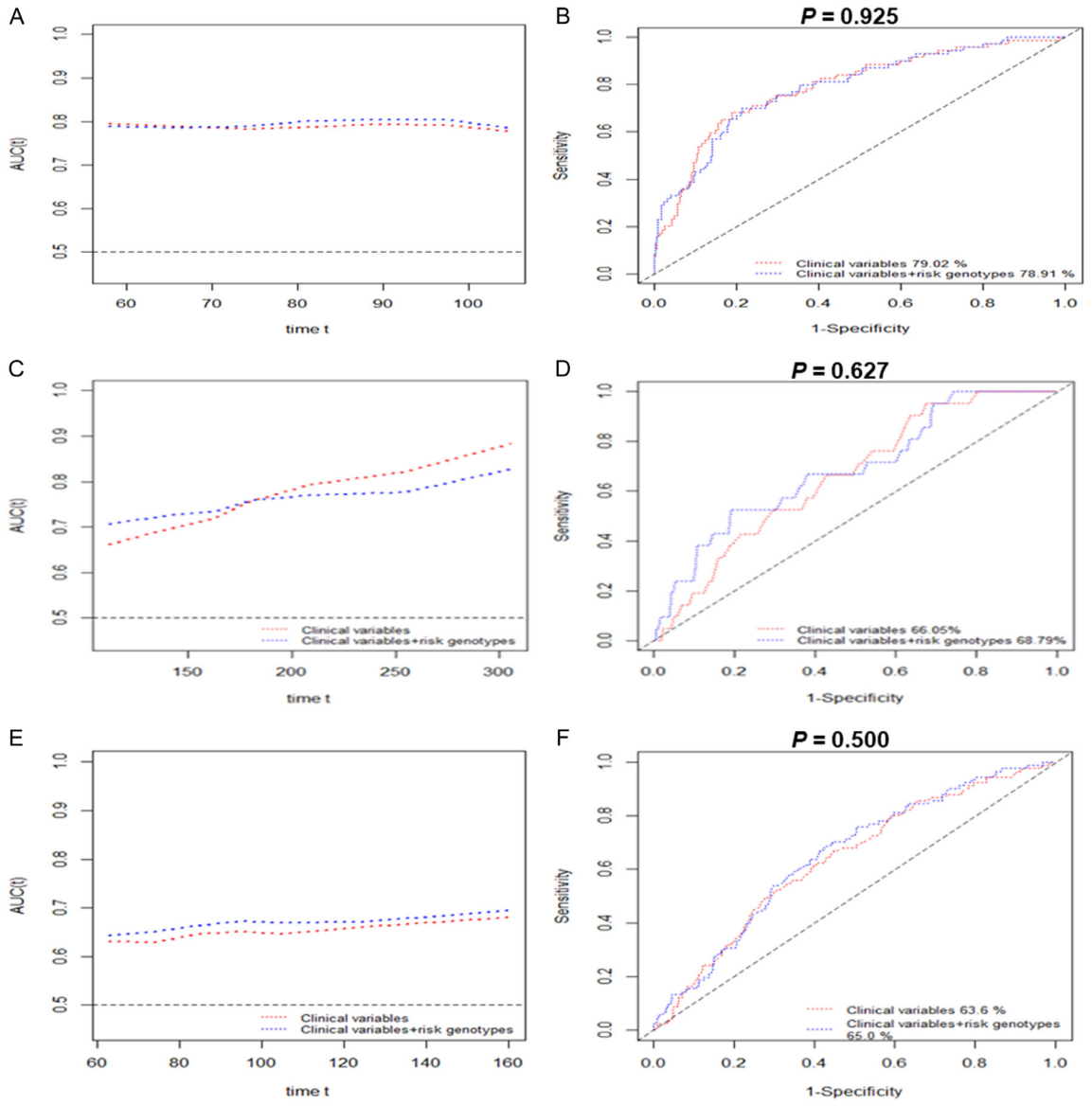

Figure S4. ROC curve and time-dependent AUC estimation for five-year CMSS prediction in CM patients. The Time-dependent AUC estimation based on clinical variables plus risk alleles in the MDACC dataset (A), NHS/HPFS dataset (C) and combined MDACC and NHS/HPFS dataset (E). ROC curves of five-year CMSS prediction in the MDACC dataset (B), NHS/HPFS dataset (D) and combined MDACC and NHS/HPFS dataset (F). Abbreviations: CMSS, cutaneous melanoma-specific survival; SNP, single-nucleotide polymorphism; AUC, area under receiver curve; MDACC, The University of Texas MD Anderson Cancer Center; NHS/HPFS, Nurses'Health Study/Health Professionals Follow-up Study; ROC, receiver operating characteristic.

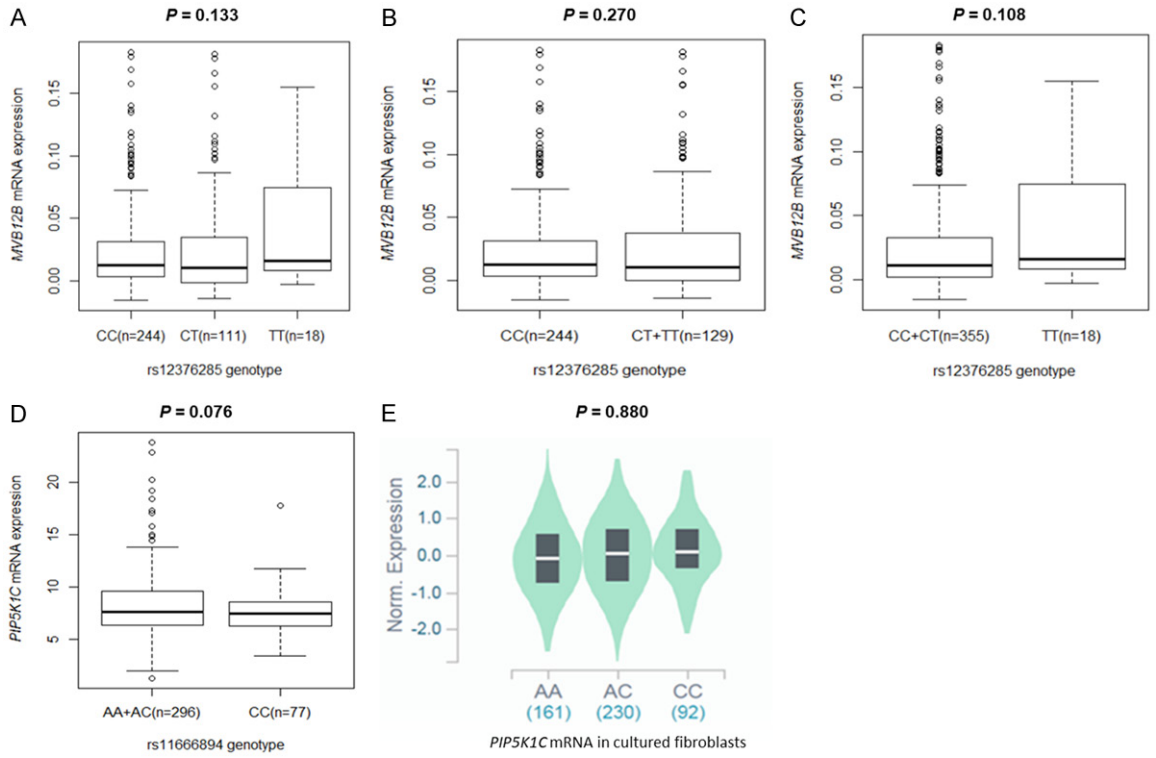

Figure S5. The eQTLs analysis for *PIP5K1C* rs11666894 *and MVB12B* rs12376285. The correlation of rs12376285 genotypes and *MVB12B* mRNA expression in the additive (A) model, the dominant model (B) and the recessive model (C) from the 1000 Genomes Project. The correlation of rs11666894 genotypes and *PIP5K1C* mRNA expression in the recessive model (D) from the 1000 Genomes Project and in the cultured fibroblasts (E) from the GTEx database. Abbreviations: eQTLs, expression quantitative trait loci; GTEx, Genotype-Tissue Expression project.

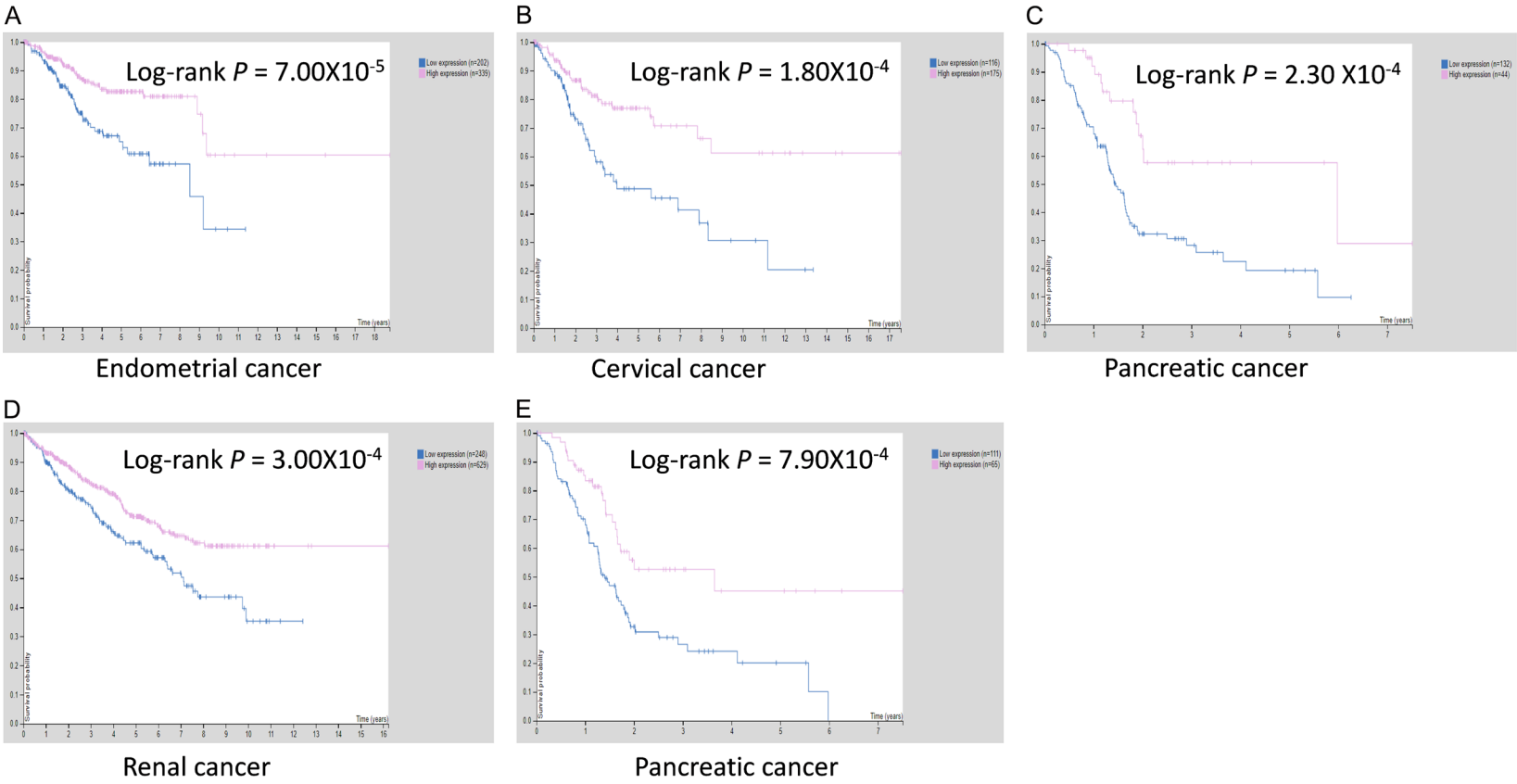

Figure S6. Association between mRNA expression and survival prediction of cancers in Human Protein Atlas database. *PIP5K1C* mRNA expression showed significant correlation with survival probability in patients with endometrial cancer (A), cervical cancer (B), pancreatic cancer (C) and renal cancer (D); the expression level of *MVB12B* mRNA was significantly associated with the survival in pancreatic cancer patients (E) based on Human Protein Atlas database.